Pure & Appl. Chem., Vol. 66, No. 12, pp. 2537–2586, 1994.
Printed in Great Britain.

INTERNATIONAL UNION OF PURE
AND APPLIED CHEMISTRY

ANALYTICAL CHEMISTRY DIVISION
COMMISSION ON RADIOCHEMISTRY AND NUCLEAR TECHNIQUES*

DETERMINATION OF VERY LOW LEVELS OF RADIOACTIVITY

(Technical Report)

Prepared for publication by

I. ZVARA[1], P. POVINEC[2] and I. SYKORA[2]

[1]Joint Institute for Nuclear Research, Dubna, Russia
[2]Comenius University, Bratislava, Slovakia

Contributor

M. SAKANOUE

Low Level Radioactivity Laboratory, Faculty of Science, Kanazawa University, Tatsunokuchi-machi, Nomi-gun, Ishikawa-ken, 923–12 Japan

*Membership of the Commission during the period (1987–93), when this report was prepared was as follows:

Chairman: 1987–91 D. C. Hoffmann (USA); 1991–93 J.-P. Adloff (France); *Vice-Chairman*: 1989–91 J.-P.Adloff (France); 1991–93 Y.-F. Liu (China); *Secretary*: 1987–93 H. R. von Gunten (Switzerland); *Titular Members*: J. Foos (France; 1987–93); K. S. Kasprzak (USA; 1987–93); Y.-F. Liu (China; 1987–91); I. Zvára (Russia; 1987–93); *Associate Members*: H. J. Ache (FRG; 1987–91); H. A. Das (Netherlands; 1987–93); R. J. H. Hagemann (France; 1987–91); G. Herrmann (FRG; 1987–91); P. Karol (USA; 1987–93); V. P. Kolotov (Russia; 1991–93); J. V. Kratz (Germany; 1991–93); S. G. Luxon (UK; 1987–89); J. Madic (France; 1991–93); W. Maenhaut (Belgium; 1987–93); H. Nakahara (Japan; 1989–93); M. Sakanoue (Japan; 1987–91); H. Sano (Japan; 1987–89); J. A. Tetlow (UK; 1989–93); Y. Zhu (China; 1991–93); *National Representatives*: N. K. Aras (Turkey; 1987–93); G. B. Baro (Argentina; 1987–91); P. Benes (Czechoslovakia; 1989–93); K. Burger (Hungary; 1987–91); J. N. Peixoto de Cabral (Portugal; 1991–93); C. H. Collins (Brazil; 1991–93); M. Sankar Das (India; 1987–89); J. J. Fardy (Australia; 1989–93); A. P. Grimanis (Greece; 1991–93); N. E. Holden (USA; 1987–93); M. J. Kostanski (Poland; 1989–91); C. Lee (Republic of Korea; 1991–93); J. O. Liljenzin (Sweden; 1989–93); B. F. Myasoedov (Russia; 1989–91); M. Peisach (Republic of South Africa; 1987–93); A. Ponka (Poland; 1991–93); K. Roessler (FRG; 1989–91); E. Roth (France; 1987–93); J. R. Gancedo Ruiz (Spain; 1991–93); T. Shiokawa (Japan; 1987–89); E. Steinnes (Norway; 1987–93); A. Verts (Hungary; 1991–93).

Names of countries given after Members' names are in accordance with the *IUPAC Handbook 1991–93*; changes will be effected in the *1994–95* edition.

Determination of very low levels of radioactivity (Technical Report)

Abstract - This evaluation of techniques, apparatus, and dedicated facilities for measurement of very low levels of radioactivity is addressed to the large community of researchers who use radioactive tracers, make activation analyses, etc. and may occasionally face the problem of measuring an activity well below the level accessible with standard commercial equipment. Emphasis is put on the instrumental gamma-spectrometric assay of complex mixtures of radionuclides, on the spectrometric measurements of alpha activities in relatively massive samples, and on counting spontaneous fission events in samples of large mass and/or volume. A list of institutions and agencies which are active in developing low-level counting methods is given.

CONTENTS

1. INTRODUCTION

Nowadays, chemists working in very different fields deal with radioactivity measurements. In addition to nuclear chemists, radiochemists, and the scientists involved in radioecological, geochemical and cosmochemical studies, there is a much larger community of researchers who, e.g., use the techniques of radioactive tracers or exploit results of activation analysis. The term "very low-level radioactivity" cannot probably be unambiguously defined through the number of decays or counts per time unit nor can it be differentiated from the terms "low-level" and "ultra low-level" counting, which are also used in the literature. On the other hand, the equipment capable of measuring very low levels (and what is more, ultra low levels) is obviously superior to some standard low-level apparatus. For these reasons, from here on we shall speak merely about "low-level" techniques, but we shall put emphasis on dedicated equipment and facilities in which "active" and "passive" measures result in a much better sensitivity for the detection of radionuclides with particular decay modes than the sensitivity of commercially available apparatus. These measures include the use of sophisticated active anticoincidence shielding (see below), the use of detectors with extremely high absolute detection efficiency and/or resolution, the capability of measuring large and massive samples, the use of special materials with low intrinsic radioactivity for the shield and other components, complex heavy passive shielding of the detector, and, finally, placing the detection equipment deep underground.

Environmentalists and cosmochemists are already quite familiar with low-level radioactivity measurements. But, occasionally, any chemist working with radioactivity may face the problem; therefore, the primary aim of this project is to provide these newcomers with some guidelines in this respect. An attempt is made to help them understand the performance of the detectors and facilities rather than construct their own equipment.

The low-level counting field is very broad and ever growing; for survey see, e.g., Refs. 1-5. Any thorough review of its current status would need frequent updating. For this reason, only representative and illustrative citations are given. Original papers on the subject are published in a number of journals, e.g., Nuclear Instruments and Methods, Journal of Radioanalytical and Nuclear Chemistry, and Applied Radiation and Isotopes. A regular international conference on low level-counting and spectrometry is held every five years in Czechoslovakia (Refs.6-9).

As part of the present project, a list was compiled of some 100 institutions and agencies from 33 countries which are active in developing counting methods for low-level activities, possess appropriate installations, and might be contacted and asked for advice.

Low-level gamma-spectrometric assay seems to be the technique of most general interest for the categories of researchers addressed in this project. In addition, we pay attention to the spectrometric measurements of alpha activity and to counting spontaneous fission (SF) in massive and voluminous samples. We emphasize large mass because, in principle, radiochemical methods are capable of concentrating alpha- and SF-active nuclides from samples of any mass to any degree, and in this way the counting problem can be reduced to the measurement of a few milligrams or less of a substance spread on an area of a couple of square centimeters. Then the high detection efficiency and the low background are much easier to achieve. Similarly the radiochemical isolation of gamma-emitting isotopes of an element may help circumvent the problems of resolving complex spectra and of lower efficiency in measuring voluminous samples. But, unfortunately, radiochemical procedures for large initial samples happen to be very tedious and time-consuming, and the chemical yield may be uncertain and/or difficult to measure. At very low levels of activity, there is a danger of contaminating the final concentrate by radioimpurities in the chemicals used for radiochemical treatment. The material to be analysed may be so rare and unique that the development of appropriate procedures for a particular sample may not be possible. For all these reasons, direct instrumental analyses of radioactivity are preferred whenever feasible.

We felt it reasonable to omit here certain topics of low-level radioactivity measurements from discussion. Thus, e.g., mixtures of beta-emitters cannot be easily analyzed by spectrometry, especially at very low levels of activity, because of the extremely broad "spectrum" of beta particles for a given beta decay energy. Hence, such emitters must be chemically separated and isolated to be determined. High-sensitivity counting of some very important low energy beta-emitters - ^{3}H, ^{14}C, ^{39}Ar, etc. - with Geiger, proportional, and scintillation counters is a specialized field which is not considered within this project. It is reviewed in Refs. 10 & 11. It may be sufficient to say that the background for beta counters is reduced in a similar way as for gamma-spectrometric measurements. Next we can mention that recent years have seen very significant progress in using "accelerator mass spectrometry" for the assay of long-lived cosmogenic radionuclides: ^{10}Be, ^{14}C, ^{26}Al, ^{129}I (which is also a fission product), etc. The accelerator (Van de Graaff, tandem, cyclotron) serves as a high resolution mass spectrometer. The system ion source plus accelerator should be capable, e.g., of separating ^{14}N, $^{12}CH_2$ and ^{14}C with the first two species being more abundant by many orders of magnitude. The accelerated ions are counted, so no true radioactivity measurement is involved and, for this reason, the technique is not discussed here. Also, chemical concentrations are, as a rule, necessary. The reader is referred to Refs. 12-14 for reviews.

In recent years, several dedicated underground facilities have been built all over the world to measure with an extremely high sensitivity some unique and rare modes of decay and also products of the nuclear reactions induced by neutrinos. Their purpose is to solve some fundamental problems of particle physics and to carry out galactic and solar neutrino studies. These caves, tunnels and mines provide excellent shielding from cosmic rays and some of them are located in rocks (or salt) with a very low level of natural radioactivity. Thus they are the best available places for low-background alpha, beta, gamma and SF-measurements. In fact, extremely low-level beta counting is used in evaluating results of some neutrino experiments. Characteristics of these underground facilities and their research programs are given in Chapter 6 of this project written by M. Sakanoue.

2. LOW-LEVEL GAMMA-SPECTROMETRY

2.1. Introduction

In this chapter we discuss the basic principles of low-level spectrometric gamma activity measurements. In the first part (2.2) we describe spectrometric characteristics of semiconductor (2.2.1) and scintillation (2.2.2) detectors, such as the energy resolution, the detection efficiency, the peak-to-Compton ratio, etc. This may help the reader in selecting "the best" detectors to solve particular problems. Then the limiting factor in increasing the sensitivity of a given detection system is the level of background radiation. This is composed of the radiation of radioactive species contained in the detector and in the surrounding materials, and is also produced by cosmic rays. It can be minimized by shielding the detection system against the external background radiation and by selecting "radiopure" construction and surrounding materials. It is, of course, necessary also to eliminate disturbances in the electrical network, which can give background pulses as well.

The second part (2.3) is devoted to the discussion of the background radiation sources (2.3.1) and to the methods of their suppression (2.3.2). Suitable shielding materials are suggested and some typical constructions of low background shields are described. Characteristics of some underground laboratories are also presented.

The third part (2.4) deals with low-level spectrometry and spectrometers as such. First, some statistical relations and formulae for spectra evaluation, for the minimum measurable activity, the detection limit, and the figure of merit are introduced (2.4.1). Further, various types of spectrometers are described (2.4.2-2.4.8) - single detector, anti-Compton, coincidence, and pair spectrometers. Some methods of energy and efficiency calibration of spectrometers for various samples are briefly mentioned (2.4.1).

The conclusion summarizes the basic principles of low-level gamma-activity measurements, suggesting the most suitable experimental arrangements for various requirements.

2.2. Gamma radiation detectors

For the detection of gamma radiation, semiconductor and scintillation detectors are most widely used (Refs. 1,15-17).

2.2.1. Semiconductor detectors. These detectors operate on the principle of a diode (usually the so-called p-i-n structure). Ionizing radiation interacting with the semiconductor material produces electron-hole (e-h) pairs, the number of which is proportional to the absorbed energy. The average energy required to produce a pair is 2.9 eV and 3.8 eV in germanium and silicon, respectively. Thus a 1 MeV photon if completely absorbed in Ge yields about 350×10^3 pairs - much more than in other detectors (Table 1). The statistical character of the e-h pair formation causes fluctuations in the actual number of the charge carriers produced. Due to some peculiarities of the mechanism of creating e-h pairs, contrary to an expectation from the Poisson distribution, the dispersion of the number of pairs is smaller than this number by the so-called Fano factor, which for germanium and silicon is 0.15.

The real pulse-height spectrum of a source of monoenergetic electromagnetic radiation observed with a semiconductor detector is a consequence of three basic processes through which the radiation interacts with matter and produces ionizing electrons: the photoelectric effect, Compton scattering, and electron-positron ($e^{\pm}$) pair production. The corresponding absorption characteristics of germanium and silicon are given in Fig. 1.

TABLE 1. Number of photoelectrons or e-h pairs formed in various materials (detectors) per MeV

Čerenkov detector	10-20
Plastic scintillator	700
Liquid scintillator	700
Stilbene	800
Anthracene	2000
NaI(Tl)	4000
Gas ionization chamber	30000
Silicon	260000
Germanium	350000

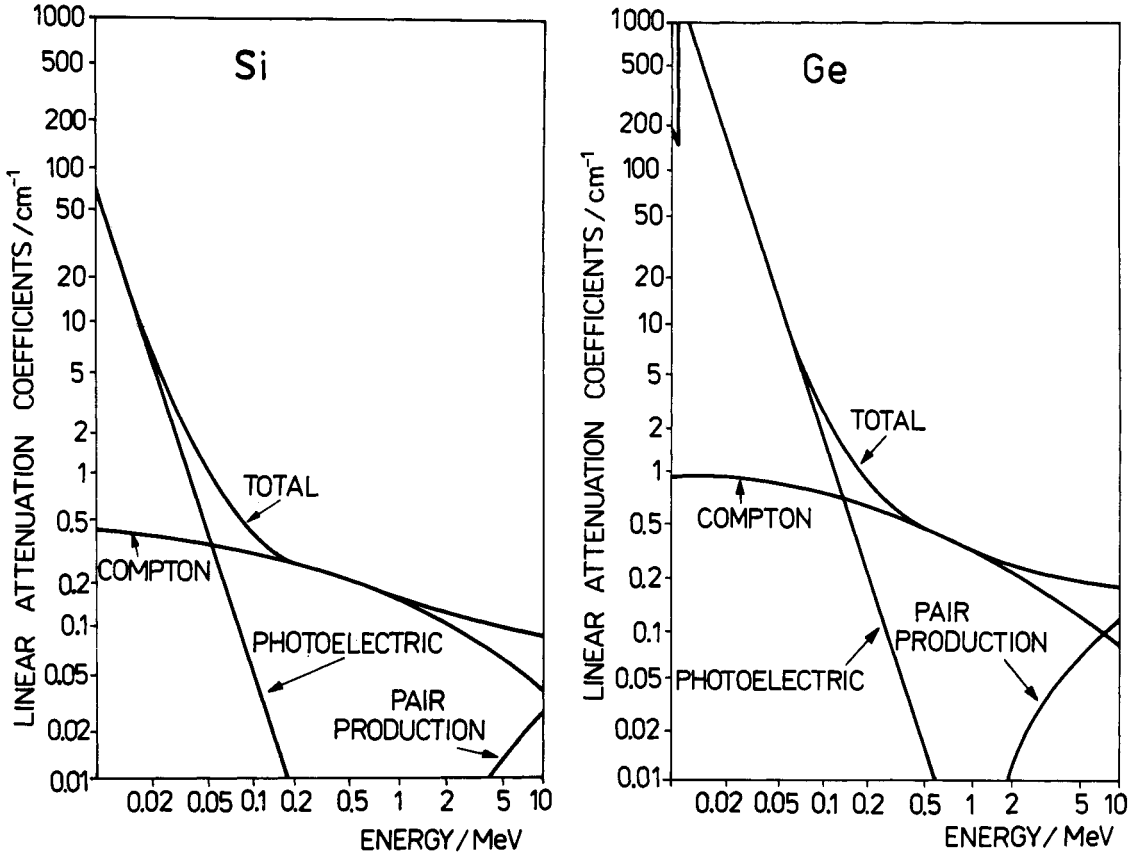

Fig. 1. Absorption characteristics of silicon and germanium

The photoelectric effect cross-section is proportional to Z^5 (Z is the atomic number of the material) and rapidly increases with decreasing energy of the incident photon. The Compton scattering cross section is proportional to Z of the scattering material, and the dependence on incident photon energy is not so strong as for the photoelectric effect. The energy of the scattered photon, E', in keV, can be expressed as

$$E' = E/\{1 + E\cdot(1 - \cos\theta)/511\},$$

and the maximum energy in the Compton continuum, the so-called Compton edge, CE, as

$$CE = E/(1 + 511/2E),$$

where E is the incident photon energy in keV.

The e^{+}_{-} pair creation is a threshold process starting at the photon energy equal to 1022 keV - the combined electron-positron rest mass. The cross section is proportional to Z^2 of the scattering material and increases rapidly above the threshold (see Fig. 1). Two 511 keV gamma quanta from the annihilation of a positron are emitted; one or both of them can escape from the detector volume. Fig. 2 illustrates the relative importance of the above mentioned mechanisms.

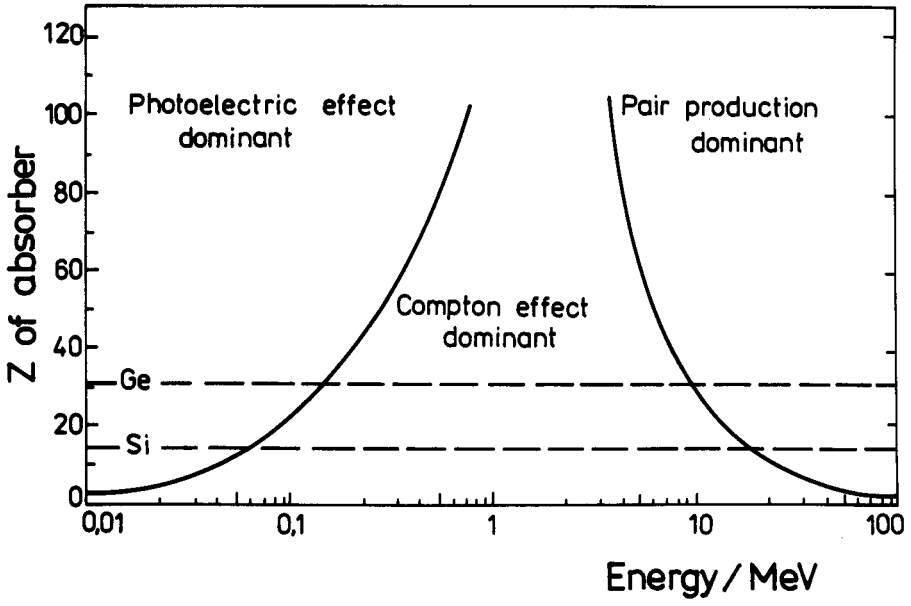

Fig. 2. Relative importance of three gamma-ray intraction processes

Semiconductor detectors are constructed mainly from germanium and silicon single crystals. (Other semiconductor materials, e.g., HgI, PbO, CdTe are currently available only as small size crystals with low detection efficiency.) Germanium has a higher atomic number than silicon and hence a higher probability of interaction for the same E. Therefore, Ge is preferable for gamma-radiation detectors. It can be prepared in a "pure" form with about 10^{14} atoms of impurities per cm^3. These impurities must be compensated for by lithium ions drifted into the germanium crystal to produce "Ge(Li)" type detectors. The "high-purity" or "intrinsic" form of germanium, HPGe, with some 10^{10} impurities/cm^3, does not require such compensation. A Ge(Li) crystal must be permanently cooled by liquid nitrogen (LN_2) to suppress mobility of lithium ions in the germanium crystal. HPGe detectors can be stored at room temperature, but must be LN_2 -cooled during operation to improve resolution.

Silicon is suitable for the construction of X-ray and alpha-particle detectors. Detectors from 0.1 to 2 mm thick are available in a pure form. Using the lithium compensation, the thickness may reach some 10 mm. The low mobility of lithium ions in silicon allows one to keep

Si(Li) detectors at room temperature without distortion of the electrical compensation.

Semiconductor detectors are produced in two geometries - planar and coaxial. Coaxial detectors are made in various configurations: closed-end, true coaxial, hole-through, and coreles. They differ in the internal electrical field and in the velocity of charge collection.

A typical Ge-detector pulse height spectrum contains several peaks; see Fig. 3. The most important and informative one is the full energy peak (FEP) of which the maximum corresponds to the incident gamma ray energy. The peak is the sum of photoelectric events, the totally absorbed multiply-scattered Compton events, and the totally absorbed pair events. The single escape peak (E-511) keV arises when one 511 keV annihilation quantum escapes from the active region of the detector. The double escape peak at (E-1022) keV originates if both annihilation quanta escape. The continuum distribution stems from many different kinds of events, primarily from Compton scattering, with the maximum (single Compton scattering) energy CE. In the low energy part of the spectrum (not shown in Fig. 3), there is a broad peak, the backscatter one, below an energy of (E-CE). It originates from large angle (150° to 180°) backscattering of gamma rays from the inactive detector material. The asymmetric shape of the full energy peak ("tailing") is principally caused by the non-uniform distribution of the traps in the sensitive volume. Other effects that shift pulses into the tail include ohmic contact noise, infrared radiation, and the crystal lattice imperfections arising from the original ingot or from radiation damage.

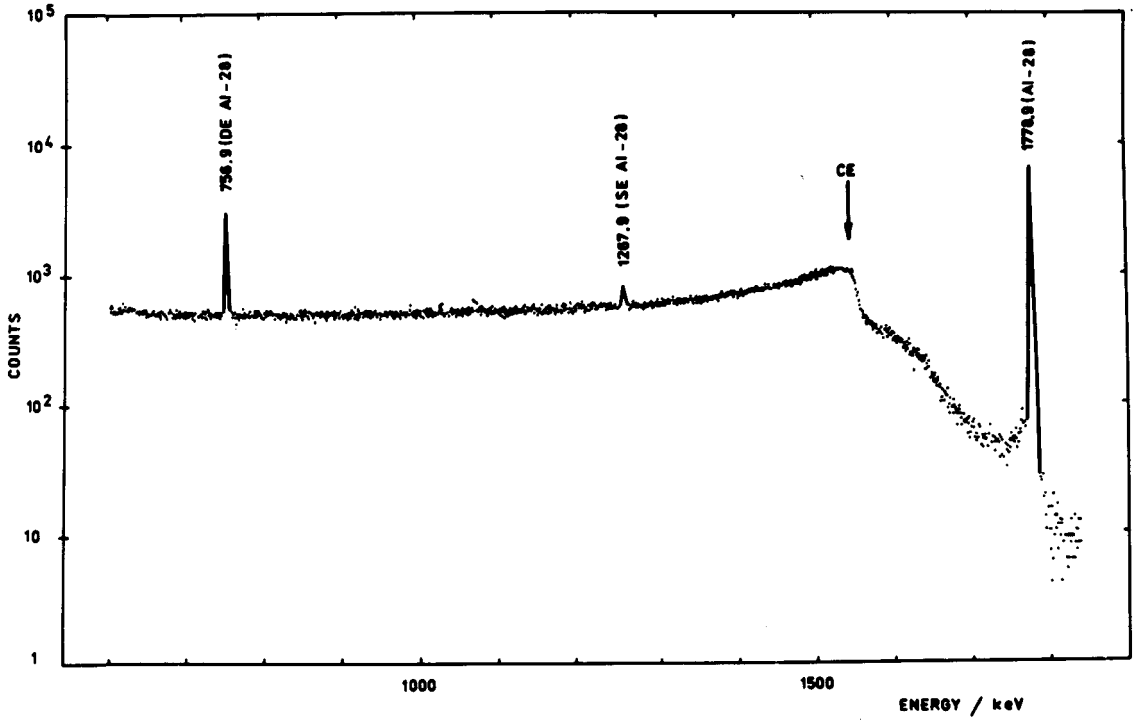

Fig. 3. Pulse-height spectrum of an ^{28}Al source, E_γ = 1777 keV, taken by a Ge(Li) detector (30 cm^3, coaxial, FWHM = 2.6 keV); from Ref. 18. CE - Compton edge, SE - single escape peak at (E_γ -511) keV, DE - double escape peak at (E_γ-1022) keV.

The spectrometric performance of a semiconductor detector is characterized mainly by the energy resolution, by the detection efficiency, and by the peak-to-Compton ratio.

The energy resolution is determined by the statistical fluctuation of the number of charge carriers produced, by the detector noise and backcurrent, and by parameters of the electronics. In order to achieve a good energy resolution, the detector must be cooled to LN_2 temperature. The energy resolution of gamma-radiation detectors is usually determined for 1332 keV gamma-rays of ^{60}Co as a full width at half maximum (FWHM) of the full energy peak. It is measured with the radioactive source at a distance of 25 cm from the detector. Ge(Li) or HPGe detectors achieve 1.5 - 2 keV FWHM resolution. Sometimes the width is given at one tenth (FWTM) or at one fiftieth of the maximum (FWFM). Very good detectors have FWTM < 1.9FWHM and FWFM < 2.65FWHM. The ratios of these peak characteristics are important for the computer analysis of complex gamma spectra.

The intrinsic energy resolution of such a detector would correspond to

$$FWHM = 2.35(\omega \Phi E)^{1/2},$$

where ω is the average energy required to create an e-h pair, Φ is the Fano factor, and E is the photon energy deposited in the sensitive volume. The real FWHM in measured spectra is larger than that due to the contribution from the noise of the employed electronic circuitry.

The energy resolution for the X-ray region is usually given for the 5.9 keV KX-ray doublet from ^{55}Fe or for the 122 keV gamma rays from ^{57}Co. Good Si(Li) detectors reach a FWHM resolution of about 140 eV for 5.9 keV X-rays.

The efficiency of semiconductor detectors in the registration of gamma rays is measured and specified for the 1332 keV full energy peak from ^{60}Co. For standard measurements, a ^{60}Co source of known activity is positioned at a distance of 25 cm from the detector. The efficiency is usually given relative to a 7.6×7.6 cm NaI(Tl) crystal at the 25 cm source-to-detector distance. The absolute efficiency of such a crystal for 1332 keV gammas in this geometry is 1.2×10^{-3}. "Large-volume" Ge(Li) and HPGe detectors have relative efficiencies of about 30%; at present "very large" detectors may achieve 100%.

The peak-to-Compton ratio is an important characteristic of gamma-ray detectors. Compton scattering is the prevailing type of interaction of 0.15 to 7 MeV gamma-rays with detector materials. In the amplitude spectrum, partially absorbed gamma-rays produce continuously distributed pulses positioned below the full energy peak (cf. Fig. 3).

The peak-to-Compton ratio is measured for the 1332 keV gamma line from ^{60}Co placed 25 cm from the detector, as the ratio of the peak height maximum to the average height of the Compton continuum between 1040-1096 keV. The value of this ratio depends on the size and type of the detector and is typically between 20 and 90.

For X-ray detectors the peak-to-continuum ratio is expressed as the ratio of the maximum height of the peak from 5.9 keV X-ray doublet of ^{55}Fe to the average height of the continuum in the 3 keV region. For good Si(Li) detectors this ratio is about 1500:1. It depends on the size and quality of the detector. A low peak-to-continuum ratio indicates a low-quality or defective detector. Poor detector performance is caused mainly by trapping and recombination effects in the detector itself.

2.2.2. Scintillation detectors. This type of gamma-radiation detector is composed of two parts: a scintillator and a photomultiplier tube

(PMT). The PMT consists of a photocathode, a focusing electrode, and of 10 or more dynodes. As a result of the interaction of gamma radiation with the scintillator, photons of light are emitted. They are first converted to photoelectrons on the photocathode, then the photoelectrons are multiplied on dynodes, and, ultimately, an output signal is produced on the anode. The PMT has a gain of 10^6 to 10^8 and can operate, depending on construction, very fast, being capable of producing 100 mA in a 5 ns pulse from one electron.

The scintillator quality is characterized by the conversion efficiency, light yield, transparency to its own radiation, and light decay time. The conversion efficiency is determined as that part of gamma-ray energy loss in the scintillator which is converted into light. The light yield is defined as the number of photons of light per energy unit absorbed in the scintillator. The scintillator must be transparent to its own light, i.e. its absorption and emission spectra must be mutually shifted. The light decay time of the scintillator is the mean life-time of excited states.

Scintillators can be divided into three groups - organic, inorganic, and gaseous. For gamma spectrometry inorganic crystals, e.g., NaI, CsI, BGO (bismuth germanate), LiI, and CaF_2 are mainly used. Plastic scintillators are also often employed, but their efficiency is much lower. Gaseous scintillators are of very limited use.

Inorganic scintillators are ionic crystals - dielectrics with a relatively wide forbidden zone (5 eV and more), separating the valence and the conduction bands; the electron states of the latter are not occupied. Ionizing radiation excites the valence electrons into the conduction band, so that holes appear in the valence band. Recombination of electrons and holes by direct transition over the forbidden zone may be realized by emitting a photon, but it cannot escape from the crystal because the emission and absorption spectra of the material are the same. Therefore, some so-called activators (Tl, Eu, etc.) are needed to create levels in the forbidden zone with a high probability of photon emission (luminiscence centres). These photons are not absorbed in the crystal and may escape. The activator concentration in the scintillator has an optimum value between 0.1-0.2%. NaI(Tl) crystals are available in large sizes, but they are hygroscopic and need a container. BGO and CsI(Tl) are not hygroscopic.

An important component of all scintillation detectors is the photomultiplier. Its quality is characterized by several parameters - quantum efficiency, radiation sensitivity, dark current, etc. The quantum efficiency at a given wavelength of light is the average photoelectric yield per incident photon, and is normally expressed as percentage. Radiation sensitivity of a photocathode is defined as the photocathode current emitted per power unit of incident radiation at a given wavelength of light (it is expressed in mA/W). An output from the PMT obtained in the absence of light input is the dark current, which is the sum of all pulses from the PMT plus an electrical leakage. For this reason, the dark count rate cannot be accurately predicted from the dark current. The latter is caused by thermoemission of electrons from the photocathode, by the ion and optical feed-back, and by the spontaneous emission of electrons from various parts of the PMT. Cooling of the photocathode may be used to decrease thermoemission. The PMT gain is very sensitive to changes in high voltage, therefore the power supply must be very well stabilized.

The PMT may be connected to the scintillator by a light guide (usually Plexiglass or NaI without activator). In this way one can decrease the background of the detector for measurements of low activities, because the PMT glass may contain radionuclides (see below). The permissible distance between the PMT and the scintillator is, however, limited by

losses of light in the light guide.

The time resolution of scintillation detectors, defined as the shortest interval between two incident particles when they are still registered as two events, is a few microseconds for inorganic scintillators whereas for the organic ones it is about 100 -10 ns. For scintillation detectors, the interval between the moment the particle hits the detector and the appearance of the output signal is shorter than that for other types of detectors. In inorganic scintillators this delay time is about 5 ns; in organic ones the delay is limited only by the electron velocity in the PMT. Special timing PMT's have delays as short as 0.2 ns. The timing properties of the the PMT are important if the scintillator is used for anticoincidence shielding (see 2.4.3).

The energy resolution of scintillation detectors is substantially poorer than that of semiconductor detectors because of the large average energy necessary to produce a photoelectron - about 1000 eV - compared with 3 eV needed to produce one e-h pair in a semiconductor (Table 1). The higher the conversion efficiency of the scintillator and the quantum efficiency of the photocathode, the better is the energy resolution. Under otherwise equal conditions the resolution is proportional to $1/\sqrt{E_\gamma}$. Usually it is given for the 662 keV gamma line of ^{137}Cs. With middle-sized NaI(Tl) crystals a FWHM resolution of 6-8% can be achieved.

The pulse-height spectrum of gamma radiation registered by a scintillation spectrometer again contains the full energy peak, the Compton continuum, and, if the energy of gamma-rays is higher than 1022 keV, the single and double escape peaks.

The detection efficiency of a scintillation detector is usually given for the FEP of 662 keV gamma-rays from ^{137}Cs. The FEP efficiency decreases rapidly with increasing gamma-ray energy because the photoelectric effect cross section goes down. For a given energy of gamma rays the FEP efficiency increases with increasing crystal size as a result of the increasing probability of the total absorption of multiply Compton-scattered gamma rays. The FEP efficiency depends strongly on the effective atomic number of the scintillator. That is why the photopeak is practically absent in the spectra from organic scintillators. The absorption characteristics of BGO and NaI scintillators are presented in Fig. 4. NaI(Tl) crystals are available with sizes up to about 50x40 cm. In very low-level counting facilities they are used both for spectrometry and for anticoincidence shielding (see below).

2.2.3. Other types of detectors. For the measurement of soft gamma rays and X-rays, proportional counters are also used, mainly when large sensitive volumes are needed. The gaseous samples being measured can be added directly to the working gas; solid samples can be put onto a foil and placed in the sensitive volume. The simplest type of proportional counter is a cylinder with one axial wire but multiwire wall-less proportional counters are also used. The measurement geometry is 2π or 4π, the detection efficiency being nearly 100%. The energy resolution (FWHM) of a cylindrical one-wire proportional counter filled with CH_4 is about 16% for the 5.9 keV X-ray doublet of ^{55}Fe. The higher the working gas pressure in the proportional counter, the higher the energy of radiation which can be measured.

2.3. Background

Peaks in gamma-radiation spectra are as a rule superimposed on a smoothly varying "background" which originates mostly from scattering

of gamma-rays of higher energies (cf. 2.4.1 and Fig. 3). Here we discuss only that contribution to the background which does not come from the radionuclides in the measured sample, so it can be reduced. It is an ultimate limiting factor in low-level radioactivity measurements.

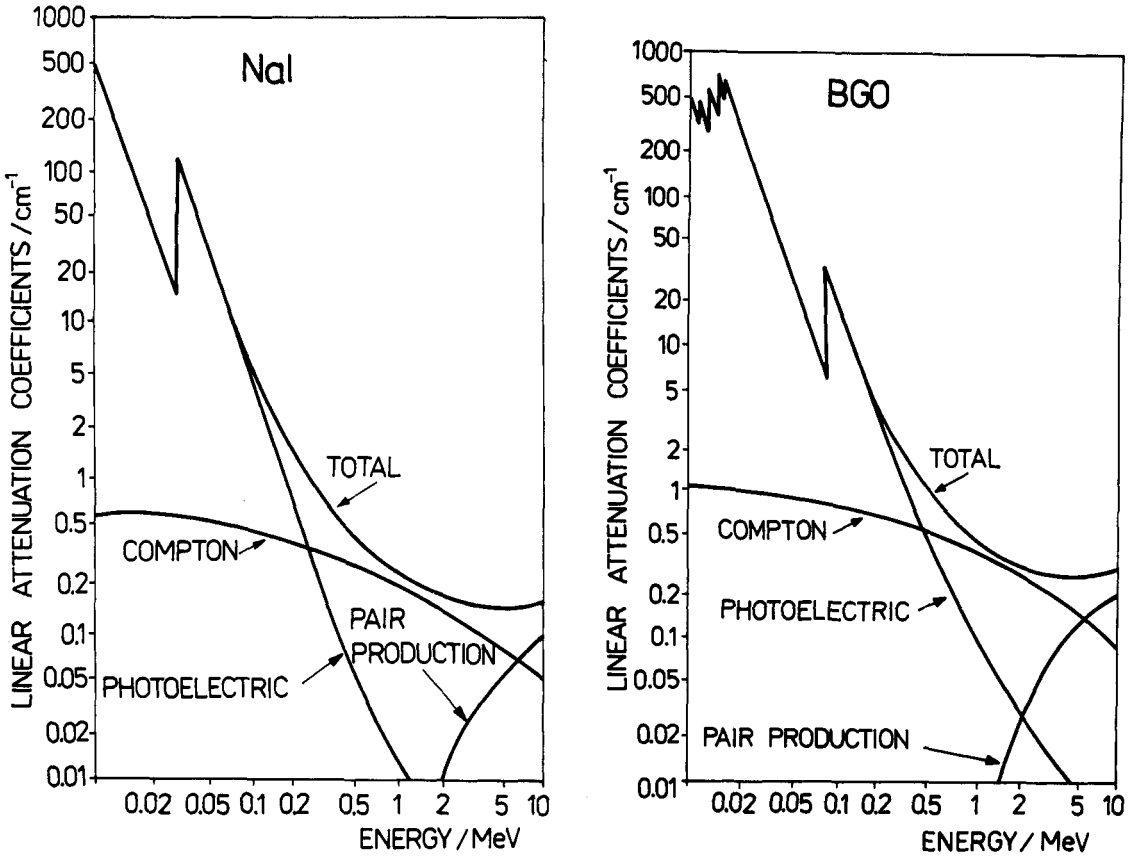

Fig. 4. Absorption characteristics of NaI and BGO

2.3.1. Sources of the background. The background in the above sense is produced by:
- activities contained in the sensitive volume and in the insensitive parts of the detector;
- activity of the materials surrounding the detector;
- radiation of cosmic origin.

The cosmic radiation at sea level can be divided, according to its penetrability, into hard (73%) and soft (27%) components. The hard component is composed mostly of charged muons (about 75% of all cosmic particles) and nucleons. Muons have a high penetrability - 50 m of water reduce their intensity only 10 times. Their contribution to the background can be supressed by placing the detection system very deep underground and by anticoincidence shielding (see below). The soft component of cosmic radiation is composed of electrons, positrons, and photons. Its intensity can be sufficiently reduced by some 10 cm of lead as the mass absorption coefficient of Pb is 0.17 cm^2/g. The intensity of the cosmic radiation varies with time and locality (solar eruptions, barometric effects, etc.). Therefore, in case of long-term measurements of very low radioactivities, simultaneous counting of background and sample is desirable (Ref. 19). Cosmic rays also produce both prompt and delayed radiation (radionuclides) when interacting with nuclei via spallation reactions; cosmic ray neutrons produce background radation through inelastic scattering and neutron capture (Ref. 20).

Radioactivity of the counting medium and the detector construction materials also contributes to the background. In gas-filled detectors the working gas brings ^{222}Rn ($t_{1/2}$= 3.8 d) and its decay products. This contribution can be reduced by purifying the gas or just by aging it for several half-lives of ^{222}Rn to let the latter decay. The materials of inorganic scintillation detectors (such as NaI(Tl), CsI(Tl)) contribute to the background mainly through the radioactivity of ^{40}K, and to a lesser extent by the radioactivity of uranium and thorium decay products. The opposite is true for BGO. The intrinsic activity of low-background crystals prepared from special pure materials is about 10 times lower than that of conventional ones. The radioactivity of semiconductor detectors is usually very low as the materials used are of high purity, but prompt radiation and radionuclides originating from cosmic ray interactions with matter may be present.

The detector construction materials - electrodes, insulators, photomultipliers, etc. - must be selected to contain the lowest possible activity. Some metals, e.g., Al, Pb, and bronze usually have a high level of radioactive impurities (Th,U) and they are not recommended for the construction of detectors. Solders also have a rather high level of radioactivity and are recommended to be prepared from radiopure tin and centuries-old lead. Electrolytic copper (especially oxygen-free) is a suitable material. Stainless steel is also good, but before use it must be checked for possible radioactive tracers, e.g., ^{60}Co. Plastics such as polyethylene, Teflon, nylon, etc. have very low intrinsic radioactivity. Glass has a relatively high radioactivity, mainly due to ^{40}K, except for quartz glass. Data on the radioactivity of some construction and other materials used in detector systems are presented in Table 2. The problem is discussed also in Refs. 21-24.

TABLE 2. Typical radioactivity of some materials (mBq/g). From Ref. 16.

	^{232}Th	^{238}U	^{40}K
Metals: Al	0.7	0.07	0.9
Ti	0.004	0.06	0.02
Cu	0.04	0.06	0.2
Ge	0.02	0.02	0.2
Fe	0.01	0.01	0.1
MgO	0.2	0.3	0.4
Pyrex glass	0.8	0.6	8
Flint glass	0.03	0.03	0.1
Polyvinyl resin	2	2	3
Apiezon grease	8	8	5
Molecular sieve	8	6	18
Epoxy resin	0.01	0.02	0.4

At the ultimate level of sensitivity, in deep underground facilities, cosmic-ray produced activities in otherwise radiopure construction materials may become important. For example, electrolytical copper is no longer suitable (Refs. 21 & 22). The problem requires special investigation in each case.

The radiation from the materials surrounding the detector system and from the earth's surface brings another contribution to the background. It comes from terrigenous, radiogenic, and anthropogenous

radionuclides. Terrigenous (primordial) nuclides- ^{238}U, ^{232}Th, ^{235}U, and ^{40}K - remain in the earth's crust from the time of nucleosynthesis because of their long half-lives ($>10^9$ years). Radiogenic radionuclides are daughter products of the terrigenous ones. All radioactive series include gaseous radon (^{222}Rn in the ^{238}U series, ^{220}Rn in the ^{232}Th series, and ^{219}Rn in the ^{235}U series) which is released into the atmosphere. From the short-lived gamma-active decay products of Rn isotopes, the most important are ^{218}Po, ^{214}Po, and ^{214}Bi. The concentration of ^{238}U in soil is about 1 ppm (10 Bq/kg plus members of the series), of ^{232}Th about 10 ppm (40 Bq/kg plus members of the series), and of potassium about 0.1-1%, i.e. 20-200 Bq/kg.

Building materials may contain relatively high concentrations of radionuclides. Table 3 shows the radioactivity of some of these materials. Dunite and quartz sand have the lowest activity. A higher activity of building materials may be also due to unsuitable filling materials; e.g., ashes from coal power stations may contain up to about 400 Bq/kg of ^{226}Ra (plus radiation of the members of the series). More data can be found in Ref. 25.

TABLE 3. The average radioactivity of structural materials (Bq/kg)

Material	^{40}K	^{226}Ra	^{232}Th
Granite	700	60	60
Sand	200	10	10
Gravel	150	10	10
Limestone	60	10	5
Marble	150	10	5
Cement	200	20	15
Brick	600	50	50
Clinker	600	60	70
Aerated concrete	400	40	30
Coal fly ash	400	100	70
Asbestos	200	10	15
Pearlite	1200	50	80
Ceramics	500	30	40

2.3.2. Shielding. The background due to external radiation may be reduced by shielding the sensitive volume of the detector. The "active" shielding will be described in more detail in 2.4.3. The "passive" shielding is based on the ability of materials to absorb ionizing radiation. Convenient is the use of high atomic number materials, e.g., Pb, W, Mo, Cu, and Fe.

Lead is used most frequently but modern lead has a relatively high radioactivity mainly from ^{210}Pb with $t_{1/2}$= 21 years, less from ^{226}Ra with $t_{1/2}$= 1622 years. It is better to use an old lead, produced some centuries ago, but it is more expensive. Iron (steel) has a lower level of radioactive impurities, but its layer must be about two times thicker if one wants to get the same absorption as with Pb. Mercury has usually a low intrinsic radioactivity, but is toxic and needs a container. Electrolytic copper is a very good shielding material but its price is high. The same is true also for W and Mo.

Neutrons pose specific problems in the reduction of background. They arise mainly from interactions of cosmic radiation with high-Z shielding materials. In lead, a high energy nucleon creates about 60 neutrons per interaction and some mesons, which also produce neutrons. A 10 cm low-Z moderator layer (paraffin, polyethylene, etc.) slows down neutrons to thermal energy during about 2 μs and then they may be absorbed in the ^{10}B (n,α) ^{7}Li reaction by adding boron into the moderator material. A smaller portion of neutrons will interact via (n,γ) reactions with the impurities of the moderator. Therefore only a thin layer of high-Z material should be placed between the moderator and the detector to suppress the prompt capture gamma-rays and bremsstrahlung.

When measuring soft gamma-rays or X-rays, characteristic X-rays created in the shield can be suppressed by absorbers with gradually decreasing (towards the detector) atomic numbers. For example, after Pb a layer of Cd is used to suppress the 72 keV X-rays of Pb, then a layer of Cu to suppress the X-rays of Cd, and finally a layer of a low Z material (e.g., Plexiglass).

2.3.3. Shielding and background characteristics of some facilities. Comparison of the performance of a 100 mm×100 mm NaI Tl spectrometer in ten shields of different construction is reported by Sobornov et al. (26). An example of a simple construction of a passive shield which is employed at the Comenius University, Bratislava, Czechoslovakia is described by Stanicek et al. (27). Its dimensions are 800x900x1720 mm, and the total mass is about 18000 kg. It is composed (starting from the outside) of a 10 mm Fe layer, 100 mm of Pb, 50 mm of Cu, 80 mm of polyethylene with boric acid (NEUTROSTOP bricks), 1 mm of Cu, and 10 mm of Plexiglass. To reduce the soft component of the cosmic radiation, the shield top is strengthened by 120 mm of iron. All materials are of modern production; no special selection has been made. The comparison of gamma background spectra (measured by a 70 cm^3 Ge(Li) detector) inside and outside the shield is shown in Fig. 5. Suppression of background lines in the energy region of 250-2750 keV is 60-340 fold and depends on the energy.

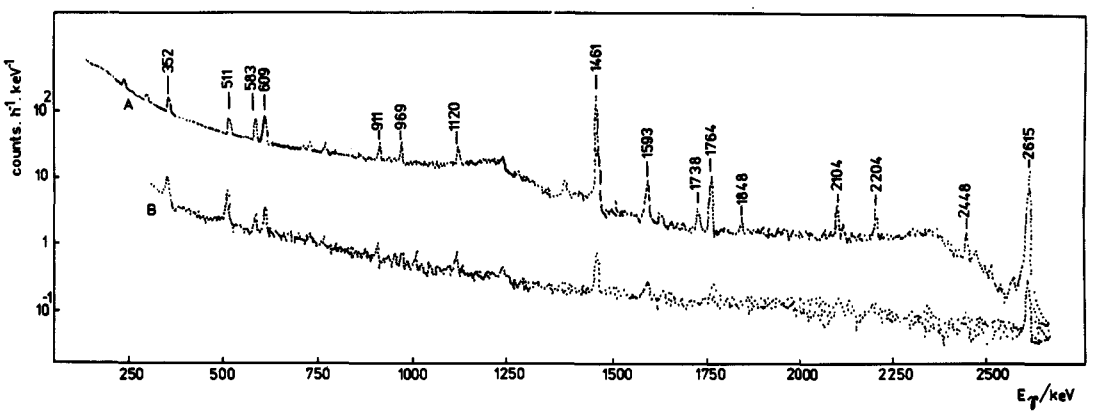

Fig. 5. Comparison of Ge(Li) background spectra outside (A) and inside (B) the shield (from Ref. 28).

Some rare decay experiments, such as the measurement of alpha-activity, spontaneous fission, the double beta decay, proton decay, etc. require suppression of the muonic component of the cosmic radiation. This is possible if the laboratory is built deep underground (see also chapter 5). A depth of about 10 m of water equivalent (m w.e.) has a positive effect in lowering the background.

At the Heidelberg (Germany) underground laboratory, at a depth of 15 m w.e., a low background Ge(Li) spectrometer is installed in a shield consisting of 24 mm of mercury in a Plexiglass container, and 72 mm of old ship iron. Some active shielding measures are also provided. The total background count rate in the energy region of 80-2060 keV is 0.075 cps. No peaks of thorium series lines are observed above the continuous background. The muonic flux is reduced only by a factor of 2-3, and its counting rate is 0.008 $cm^{-2}s^{-1}$ (Ref. 29).

At the underground laboratory in Bern (Switzerland), situated at a depth of 70 m w.e., muon, gamma, and neutron fluxes are reduced by factors of 11, 6, and 8, respectively (Ref. 30). At this laboratory, ^{39}Ar (for ice and groundwater dating), ^{37}Ar, ^{3}H, and ^{14}C concentrations in the atmosphere have been measured by proportional counters.

The underground laboratory at Rossendorf (Germany), 125 m w.e. deep, is mainly used for activation analysis of pure materials. The cosmic radiation is reduced here aproximately by a factor of 40 (Ref. 31).

The underground laboratory in Freiburg (Germany) is located at a depth of 340 m w.e.. Ge(Li) and NaI(Tl) spectrometers, and a proportional counter for tritium measurements are installed here. The background count rate, measured with a 10 cm^3 Ge(Li) detector, is 141, 11, and 0.009×10^{-4} cps per 10 keV interval at 1 MeV, 2 MeV, and 3 MeV, respectively (Ref. 32).

The underground laboratory in the Solotwino salt mine (Ukraine) is situated at a depth of 1000 m w.e. The cosmic ray flux is reduced by a factor of 10^4. NaI(Tl) and Ge(Li) spectrometers in a shield are installed there. The reduction of NaI(Tl) background in the energy region 0.1-3 MeV is 30-40-fold in comparison with a surface laboratory. The Ge(Li) background reduction is 55-825-fold in the energy region 0.2-3 MeV (Ref. 33); cf. Fig. 6.

The Baksan underground laboratory (Caucasus, Russia) includes several locations at various depths. The first one is situated at 660 m w.e., and low-background gamma spectrometers in a passive shielding are installed here to measure the ^{150}Nd double beta decay. The background of a liquid scintillator is about 0.02 cps/kg for energies ≥ 1 MeV, and for a low-background NaI(Tl) detector it is 0.32 cps/kg in the 0.2-3 MeV region. The largest laboratory located at 850 m w.e. houses a neutrino scintillation telescope (Ref. 34).

The Grand Sasso underground laboratory (Italy) is located under the central Apennine chain at a depth of about 3500 m w.e. The muonic flux is about 16 $m^{-2}d^{-1}sr^{-1}$; the environmental gamma rate measured with a 25% relative efficiency Ge(Li) detector, is 60, 19, 1.9, and less than 0.05 $keV^{-1}h^{-1}$ at 0.5 MeV, 1 MeV, 2 MeV, and 3 MeV, respectively (Ref. 35).

The Mont Blanc underground laboratory is situated at a depth of 5000 m w.e. Two specially constructed large-volume Ge(Li) detectors for the measurement of the ^{76}Ge and the ^{130}Te double beta decays were installed here. The cosmic muon flux is reduced about 10^4 times to less than 0.7 $m^{-2}d^{-1}sr^{-1}$, but the radioactivity of the Mont Blanc rock is quite high. The environmental gamma rate measured with a 25% relative efficiency Ge(Li) detector is 570, 160, 19, and 0.046 keV h^{-1} at 0.5 MeV, 1 MeV, 2 MeV, and 3 MeV, respectively (Ref. 35).

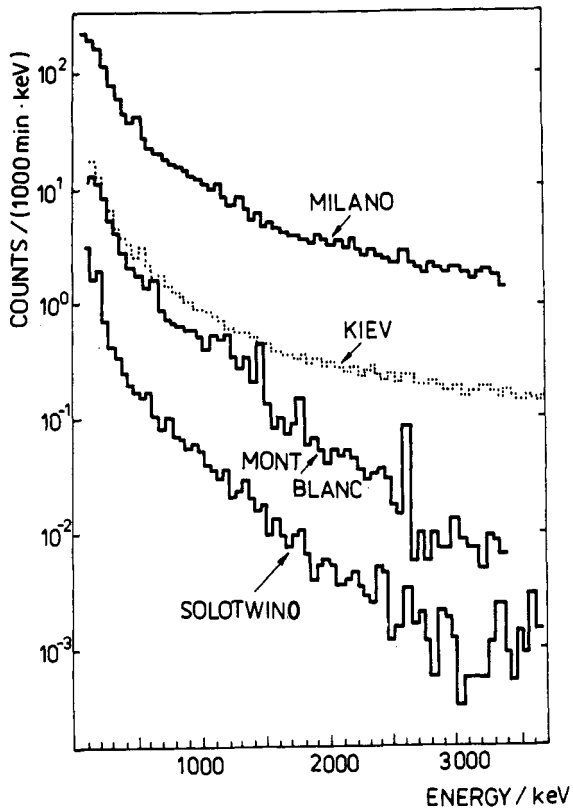

Fig. 6. Comparison of Ge(Li) background spectra in above ground (Milano, Kiev) and underground (Mont Blanc, Solotwino) laboratories; from Ref. 33.

2.4. Low-level gamma-ray spectrometers

2.4.1. Gamma-ray spectra evaluation. The goal of gamma-ray spectrometry is the determination of the energies and intensities of individual gamma-lines and the determination of unknown concentrations of radionuclides in different samples. Analysis is accomplished by resolving the complex gamma-ray spectrum into its components.

The energy is estimated from the position of the FEP in the spectrum, and the intensity is evaluated from the net area under the peak. The gamma-ray spectra are recorded by a multichannel analyser and usually processed by a computer, but a preliminary visual inspection of the spectrum is very useful in choosing an optimal method of evaluating the spectrum. If the measured spectra have poor counting statistics, their statistical properties can be improved using a smoothing technique. It is assumed that the smoothed values follow more closely the correct average spectrum shape, and different peak parameters, e.g., areas and positions can be, in principle, determined with a better precision. All smoothing techniques for gamma-ray spectra are based on the linear transformation of the measured data. They are divided into three categories - Fourier transform, least-squares adjustment of a polynomial, and digital filtering (Ref. 36).

The multichannel gamma-ray spectrum consists of peaks superimposed on a smoothly varying background formed mainly by Compton scattered gamma rays. To obtain the net "area" (in counts per time unit) under the peak, S, the background or the Compton base, B, is subtracted from the peak area. As illustrated in Fig.7, the number of channels used for the peak area calculation, k, is not necessarily the same as the number

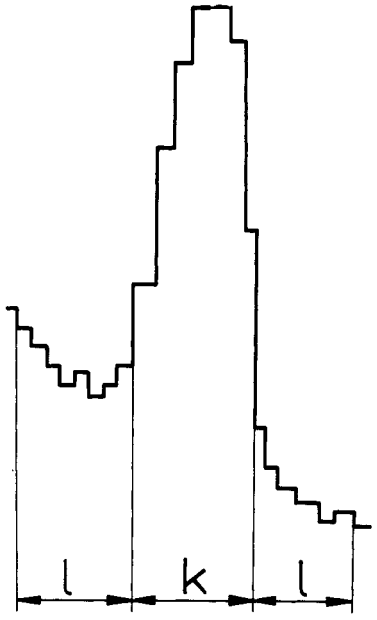

Fig. 7. Estimation of the net peak area; see text.

of channels used to estimate the background, l. Let S_n be the number of counts in the k channels of the peak area, B_i,B_j be the contents of the background channels on the left and right sides of the peak, respectively .Then we have for the net peak area

$$S = \sum_{n=1}^{k} S_n - \frac{k}{2l}\left(\sum_{i=1}^{l} B_i + \sum_{j=1}^{l} B_j \right).$$

Its variance, obviously, is

$$\sigma_S^2 = \sum_{n=1}^{k} S_n + \left(\frac{k}{2l}\right)^2 \left(\sum_{i=1}^{l} B_i + \sum_{j=1}^{l} B_j \right) \quad \text{or}$$

$$\sigma_S^2 = S + \frac{k}{2l}\left(\frac{k}{2l} + 1\right)\left(\sum_{i=1}^{l} B_i + \sum_{j=1}^{l} B_j \right) \quad \text{or}$$

$$\sigma_S^2 = S + B\left(\frac{k}{2l} + 1\right).$$

The uncertainty of the result - the confidence limits based on Poisson statistics - can be given as $\pm n\sigma$. For example, if n=1, the probability that the correct result is in the error interval is 68.3%, similarly it is 87.5% for n=2, 98.8% for n=2.5, and 99.73% for n=3.

In very low-level activity measurements the counting time, t, should be long. Therefore it is convenient to optimize the measuring time for sample and background counting. Suppose that B originates solely from the detector background. Then from the minimization of the standard deviation, $\sigma = \sqrt{(S+B)/t+B/t}$, we find the optimal ratio of the time of

measurement of the sample, T_S, and the time of measurement of the background, T_B, to be

$$T_S/T_B = \sqrt{(S+B)/B}.$$

Denoting $T = T_S + T_B$ and $K = \sqrt{(S+B)/B}$, we have (Ref. 37)

$$T_S = TK/(1+K) \text{ or } T_B = T/(1+K).$$

Statistical measures for use in gamma-ray spectrometry were discussed in detail by Bucina and Malatova (38) starting with the concepts developed by Currie (39) and other authors (Refs. 40 & 41).

The minimum measurable activity (Ref.38) or the determination limit (Ref.39), L_Q, is a limit above which the activity is quantitatively measurable with an acceptable uncertainty. It can be expressed as

$$L_Q = (n^2 + 2n\sigma\sqrt{tB})/(t\varepsilon I_\gamma \sigma^2),$$

where I_γ is the emission probability of the (particular) gamma quantum per decay and ε is the FEP efficiency.

The minimum detectable activity (Refs. 38 & 40) or the detection limit, L_D, is a hypothetical activity, which if measured will give a signal being not found significant with only a small risk of error. This limit is

$$L_D = \{n^2 + 2n\sqrt{B[(k/2l)+1]}\}/(t\varepsilon I_\gamma).$$

The L_D values from this formula evaluated for the 95% confidence interval are close to the numerical values of the more pragmatic 3σ criterion.

If interfering peaks are present in the background spectrum, the detection limit is

$$L_D = \{n^2 + 2n\sqrt{B[k/2l)+1]} + P + \sigma_P^2\}/(t\varepsilon I_\gamma),$$

where P is the net area of the interfering peak in k channels estimated from the background spectrum, and σ_P^2 is the variance of the estimate.

Care must be exercised in extending the derived formulations to ultra low-level gamma-ray spectrometry. In most cases only one sample count is made due to very lengthy counting times involved. Also, each sample has its own "self-background", and no well known background exists for a given detector under routine working conditions as it is influenced by Rn daughters present in the air, etc.

The quality of a spectrometric system, i.e., its ability to detect a gamma activity in the presence of background (interference) from various sources, is often characterized by a figure of merit, $F = F(E)$. This is usually expressed as the FEP detection efficiency devided by the square root of the background.

Interferences may arise not only from the intrinsic background of the spectrometer but also from the Compton continuum of high energy gamma-ray emitters, if they are present in the source. In the case of two (or more) emitters in the source while $E_2 >> E_1$, Cooper (42) proposed the figure of merit in the form (see also Ref. 28)

$$F(E_1) = \frac{\varepsilon(E_1)}{\{r(E_1)[B_{C2}(E_1) + B_N(E_1)]\}^{1/2}},$$

where r is the energy resolution, B_{C2} is the contribution to the continuum under the peak of E_1 due to the higher energy rays , and B_N is the background of the spectrometer. All these parameters are energy-dependent. Measurements of F for a number of detectors under various conditions were reported in Ref. 42.

The value of the figure of merit can be increased by using
- detectors with a high peak efficiency and the optimal sample-detector geometry;
- detectors with high resolution;
- coincidence detection systems to obtain "clean" spectra;
- high-purity materials for detector construction and passive shielding;
- active shielding.

2.4.2. Single detector spectrometer. This is the simplest type of gamma-spectrometer, usually composed of an NaI(Tl) or semiconductor crystal. The NaI(Tl) detector has a higher detection efficiency but a substantially poorer energy resolution and higher background when compared with a semiconductor detector. For measurements of samples with just a few peaks in their spectra, NaI(Tl) may be used. But, in general, it is better to use semiconductor detectors as their efficiency can be 60% of that of a 7.6×7.6 cm NaI(Tl) crystal while their energy resolution is about 40 times better. The basic necessary electronic circuitry consists of a high voltage power supply, a linear amplifier, an analog-to-digital convertor, and a multichannel analyser.

The dependence of the peak position (channel number) on the energy of gamma rays is nearly linear. This may be used in a narrow energy interval where the nonlinearity of the measuring device can be neglected. While just two points are needed to construct a straight line, the calibration will be more accurate if more points are used. The accuracy of the calibration is given by an error in the calibration peak position and by the accuracy of the particular reference energy. In the simplest case of an isolated Gaussian peak above near-zero background, we may estimate the energy uncertainty due to a statistical error in the peak position as

$$\Delta E = \mathrm{FWHM}/(2.36\sqrt{S}).$$

Some long-lived radionuclides suitable for the energy and efficiency calibrations of X-ray and gamma-ray detectors are listed in Tables 4 and 5, respectively.

The detection efficiency (see Fig. 8) depends in a rather complicated manner on the energy of incident gamma radiation, on the type, size and shape of the detector, on the source-to-detector distance, and on the source radial position. The efficiency may be influenced by the dimensions (Ref. 45) and composition of the radiation source, and by the absorption of the radiation in the source as well as in the surrounding materials. For the purposes of routine gamma spectrometry, the photopeak efficiency is obviously of utmost interest. It may be determined by the calculation or measurement of a set of suitable standards (Tables 4 and 5) with known absolute activity.

TABLE 4. Long-lived radioactive sources suitable for the energy and efficiency calibrations of X-ray detectors (see Refs. 43 & 44 for more data).

Nuclide	Half-life	Photon energy/keV	Absolute no. of photons emitted per 100 decays
^{54}Mn	312.6±0.8 d	5.4055 ($K_{\alpha 2}$)	7.43±0.21
		5.4147 ($K_{\alpha 1}$)	14.7±0.4
		6.00 (K_{β})	2.94±0.1
^{55}Fe	2.72±0.03 y	5.88765 ($K_{\alpha 2}$)	8.2±0.7
		5.8975 ($K_{\alpha 1}$)	16.3±0.12
		6.49 (K_{β})	3.3±0.3
^{57}Co	271.2±0.6 d	6.3908 (K_{α})	16.5±0.5
		6.4038 ($K_{\alpha 1}$)	32.5±0.8
		7.06 (K_{β})	6.56±0.2
		14.4147 (γ)	9.54±0.13
		122.063 (γ)	85.59±0.19
		136.476 (γ)	10.61±0.18
^{65}Zn	244.5±0.1 d	8.0278 ($K_{\alpha 2}$)	11.5±0.3
		8.0478 ($K_{\alpha 1}$)	22.6±0.5
		8.94 (K_{β})	4.61±0.13
		1115.52 (γ)	50.75±0.1
^{109}Cd	453±2 d	2.98 (L_{α})	11±4
		3.24 (L_{β})	
		21.9903 ($K_{\alpha 2}$)	29.1±1.0
		22.1629 ($K_{\alpha 1}$)	55.1±1.8
		25.0 (K_{β})	17.8±0.7
		88.037 (γ)	3.79±0.11
^{137}Cs	30.02±0.15 y	4.46 (L_{α})	1.1±0.3
		4.99 (L_{β})	
		31.8171 ($K_{\alpha 2}$)	2.11±0.07
		32.1936 ($K_{\alpha 1}$)	3.90±0.12
		36.4 ($K_{\beta 1}$)	1.13±0.10
		37.3 ($K_{\beta 2}$)	0.29±0.03
		661.66 (γ)	85.0±0.4

Table 4 (contd.)

^{139}Ce	137.66±0.05 d	4.64 (L_α)	13±4
		5.21 (L_β)	
		33.033 ($K_{\alpha 2}$)	23.7±0.8
		33.4413 ($K_{\alpha 1}$)	43.7±1.4
		37.8 ($K_{\beta 1}$)	16.0±0.6
		38.73 ($K_{\beta 2}$)	
		168.85 (γ)	79.9±0.1
^{207}Bi	33.4±0.8 y	2.346 ($M_{\alpha 1}$)	
		2.443 ($M_{\beta 2}$)	
		10.5 (L_α)	35.0±2.0
		12.62 (L_β)	$L_1:L_\alpha:L_\beta:L_\gamma$=5.5:43.5:42.4:8.6
		14.76 ($L_{\gamma 1}$)	
		72.8042 ($K_{\alpha 2}$)	22.8±0.5
		74.9694 ($K_{\lambda 1}$)	38.6±0.7
		84.92 ($K_{\beta 1}$)	17.1±0.4
		87.343 ($K_{\beta 2}$)	
		569.67 (γ)	97.8±0.5
		1063.62 (γ)	74±3
		1442 (γ)	0.147±0.02
^{241}Am	431±4 y	3.3 (M_α)	6.35±0.60
		13.945 ($L_{\alpha 1}$)	13.3±0.4
		13.758 ($L_{\alpha 2}$)	
		16.837 ($L_{\beta 2}$)	19.3±0.7
		17.74 ($L_{\beta 1}$)	
		20.77 ($L_{\gamma 1}$)	4.93±0.21
		59.536 (γ)	35.5±0.3

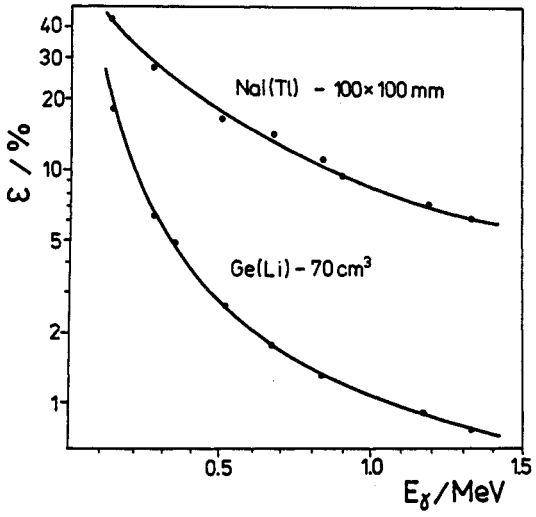

Fig. 8.
FEP efficiencies for NaI(Tl) and Ge(Li) detectors; from Ref. 28.

TABLE 5. Long-lived radioactive sources suitable for the energy and efficiency calibrations of gamma-ray detectors (see Refs. 43 & 44 for more data); weak transitions are not included.

Nuclide	Half-life	Energy/keV	No. of photons per 100 decays
^{22}Na	950.34±0.13 d	1174.5	99.94±0.02
^{54}Mn	see Table 4		
^{57}Co	see Table 4		
^{60}Co	5.272±0.002 y	1173.2	99.91±0.02
		1332.5	99.9989±0.0006
^{109}Cd	see Table 4		
^{137}Cs	see Table 4		
^{144}Ce	284.9±0.5 d	80.1	1.49±0.7
		133.5	11.09±0.02
		696.5	1.32±0.01
^{152}Eu	4892.3±8.2 d	121.8	28.4±0.3
		244.7	7.48±0.12
		344.3	26.58±0.19
		411.1	2.23±0.02
		443.9	3.09±0.04
		778.9	12.9±0.17
		867.4	4.15±0.08
		964.1	14.43±0.19
		1085.9	9.90±0.14
		1089.7	1.71±0.02
		1112.1	13.53±0.19
		1212.9	1.39±0.02
		1299.1	1.62±0.02
		1408.0	20.85±0.06
^{241}Am	see Table 4		

The dependence of the detection efficiency of a semiconductor detector on the gamma radiation energy in the range 200-2000 keV is nearly linear when plotted on a log-log scale. For a wider energy interval this dependence is rather complicated. The efficiency can be calculated using various methods (Monte Carlo computer simulation, numerical integration, etc.) with a relative uncertainty of about 5%. For practical gamma spectrometry it is convenient to determine the

efficiency experimentally. The FEP efficiency is evaluated from the measured gamma-ray peak of a standard source using the relationship

$$\varepsilon = N/(I_\gamma A D_s D_a),$$

where N is the net area of the FEP per time unit, A is the activity of the standard source, and D_s and D_a are the corrections for summing and self-absorption, respectively.

FEP efficiencies are important at energies below 4 MeV. With a higher gamma-ray energy, pair production increases, and single and double escapes begin to play a significant role. Then the single and double escape efficiencies are also needed. The uncertainty of the experimentally determined FEP efficiency depends on the method of the determination of N, on the quality of the standard sources used, on the geometry of measurements, on the method of interpolating $\varepsilon(E)$ and on the correction for coincidence summing. The coincidence summing happens due to the simultaneous detection of gamma quanta emitted in a cascade (γ_1 follows γ_2 in a time shorter than the resolving time of the detection system). These quanta may sum up via coinciding full energy absorption and form the sum peak with the energy E_1+E_2, but partially absorbed gamma quanta may also be summed and the resultant pulses may spread over a wide energy interval. The correction, N_c, coming from the coincidence summing of two cascade gamma-quanta can be estimated according to the relation (Ref. 46)

$$N_c = N_1[1 - \varepsilon_2^T(E_2)\ W_{\gamma 1\gamma 2}/(1 - \alpha^T_2)],$$

where N_1 is the net area of the FEP for γ_1 (per time unit), ε_2^T is the total efficiency for γ_2 rays, $W_{\gamma 1\gamma 2}$ is the angular correlation factor (usually less than 10%), and α_2^T is the total conversion coefficient for γ_2. The coincidence summing probability strongly depends on the measurement geometry. For a close geometry, the correction may exceed 30%. The summing correction for the source-to-detector distance greater than 20 cm is usually negligible.

The effect of coincidence summing may be used for absolute activity determination (Ref. 17). Suppose that a radionuclide decay is accompanied by emitting two gamma quanta in cascade. Then the counting rate in the FEP of γ_1 can be expressed as

$$N_1 = A\varepsilon(E_1)[1-\varepsilon(E_2)].$$

Similarly, for E_2

$$N_2 = A\varepsilon(E_2)[1-\varepsilon(E_1)].$$

The deficit in the number of counts is the same for both FEPs, and is equal to the number of counts in the sum peak

$$N_s = A\varepsilon(E_1)\varepsilon(E_2).$$

The total count rate (in the whole spectrum) is

$$N = A\ \{1-[1-\varepsilon(E_1)][1-\varepsilon(E_2)]\}.$$

The activity then is

$$A = N + N_1 N_2 / N_s.$$

The absolute activity can be determined using one detector and estimating the net areas of γ_1 and γ_2 FEPs, and the total number of counts. A problem is the interpolation of counts at the beginning of the spectrum for the determination of the total number of counts. If the cascade gamma quanta are angularly correlated, the appropriate correction must be considered.

Interpolating $\varepsilon(E_\gamma)$ for a semiconductor detector in the energy interval 200-2000 keV is relatively simple. One can use the relation

$$\varepsilon(E_\gamma) = a_o E_\gamma^{-a_1},$$

where a_o and a_1 are constants determined by fitting the measurements. The natural generalisation of this expression is a polynomial in log-log representation

$$\log[\varepsilon(E_\gamma)] = \sum_{i=1}^{n} a_i\ (\log E_\gamma)^i,$$

which is often applied in spite of that this type of a function has no physical significance. The number of free parameters a_i need not exceed seven. Fig. 9 shows an example of fitting.

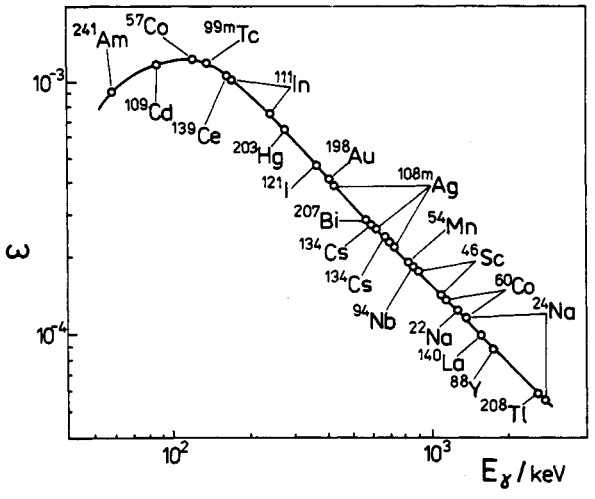

Fig. 9. FEP efficiency calibration of a 60 cm^3 Ge(Li) detector; from Ref. 47. The full line is the result of fit with sixth-order polynomial in log-log scale (Ref. 48).

Semiconductor detector efficiency interpolations can also be based on the approximation of measured data with suitable semiempirical functions with some free parameters. Their values are again obtained by least-square fitting of calibration data. Based on the physical processes of interaction of gamma radiation with semiconductor detectors, the formula is usually written as follows (Refs. 49 & 50):

$$\varepsilon(E) = a_1 \exp(-d_{Al}\mu_{Al}) \exp(-a_2\mu)\{[1-\exp(-a_3\mu)]\times$$
$$\times[(\theta/\mu + a_4(\xi+\psi)\exp(-a_5 \ln E - a_6(\ln E)^2)]\},$$

where $\exp(-d_{Al}\mu_{Al})$ is the attenuation factor for the detector window, $\mu(E)$, $\theta(E)$, $\xi(E)$ and $\psi(E)$ are cross-sections for full absorption, photoelectric effect, Compton scattering, and pair production, respectively. $\exp(-a_2\mu)$ reflects the attenuation of primary radiation in the dead volume of the detector; a_2 represents the effective thickness of the dead layer of the detector; $[1-\exp(-a_3\mu)]$ is the probability that an incoming photon will interact with full or partial loss of energy; a_3 represents the effective thickness of the detector; $[1-\exp(-a_3\mu)]\theta/\mu$ is the photoelectric effect probability; $[1-\exp(-a_3\mu)]a_4(\xi+\psi)\phi(E)$ is the probability of multiple Compton scattering and pair production, where $\phi(E)=\exp(-a_5 \ln E - a_6(\ln E)^2)$ is the correlation function for multiple scattering.

The precision of the interpolated FEP efficiencies may be about 1% or better in a wide energy interval. The experimentally determined FEP efficiencies for single gamma ray energies, measured under ideal conditions (a large source-to-detector distance, well calibrated low-mass standards), may achieve precision better than 1%. Because the uncertainty comes from the combination of squared errors of all factors, and the interpolation brings an additional error, the interpolated FEP efficiencies can be determined with a precision of about 1.5-2% in an ideal situation and in the energy interval 200-2000 keV. Efficiencies for the energies outside this range can be determined with a lower precision. Some of the problems involved in fitting ε vs. E are discussed in a recent paper (Ref. 51); Baba (52) calculated ε values using a Monte Carlo technique.

Environmental problems in which gamma-ray spectrometry is used may require large-volume samples. If we want to determine efficiencies experimentally, the preparation of a sufficient number of standards that fulfill all requirements is practically impossible. Here the difficulties are due not only to the diversity of samples, but also to the inhomogeneity of the prepared powder standards. The solution lies in using a standard measurement geometry. In this case, samples of a volume larger than the standard container cannot be used. This latter difficulty can be overcome by dividing the sample into smaller containers, all with the same measurement geometry, that symmetrically surround the detector . The detection efficiency is determined for one container and then multiplied by their number. The semiempirical approach can also be used to determine the efficiency for large-volume sample detection. The calculation can be made for substitution of the real detector by a point detector. For the FEP efficiency one can write (Ref. 53)

$$\varepsilon(E) = [GE^{-\alpha}/(H+h_o)^{\beta}]\exp(-\mu h),$$

where G, α, and β are constants, H is the height of the sample, h is the distance between the place of gamma ray creation and the top of the detector, h_o is the distance between the top and the so-called centre of detector, and μ is the mass attenuation coefficient for the sample.

Results for cylindrical samples with $H > 2$ cm agree with the experiment. For cylindrical samples with $H < 2$ cm the efficiency was calculated from the experimentally measured field of efficiencies for point sources.

Because of the adsorption of radiation in thick samples, the thickness, d, of the sample has an "optimal" value of about $1/\mu$ to $2/\mu$, as increasing the thickness above this level practically does not improve the detection limit. This is evidenced by Fig. 10. The factor $[1-\exp(-\mu d)]/(\mu d)$ characterizes the overall efficiency of detection of the activity present in the sample; it strongly decreases at $\mu d > 2$. On the other hand, consistently, the factor $[1-\exp(-\mu d)]$, to which the counting rate from the sample is proportional, only slightly increases for $\mu d > 2$ and has a limit.

To account for the gamma ray self-absorption effects experimentally, one must spike part of the sample being assayed by the measured radionuclide. Cutshall *et al.* (54) described a simpler procedure: the efficiency is determined only for some calibration material by spiking, and then the transmission of the radiation from a (sealed) disk source of the radionuclide through the unspiked calibration material and through the sample is measured. A simple formula allows calculation of the result. A detailed evaluation of the technique was published by Joshi (55 & 56).

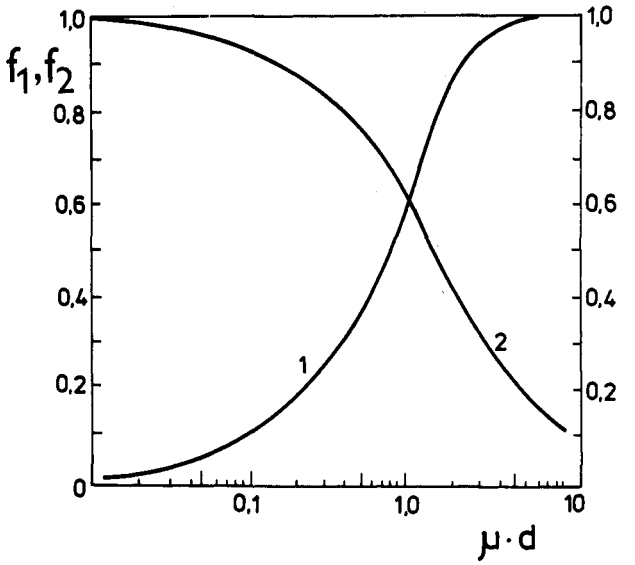

Fig. 10. On the self-absorption of gamma rays in thick samples. 1 - the factor $f_1 = [1-\exp(-\mu d)]$; 2 - $f_2 = [1-\exp(-\mu d)]/(\mu d)$.

For large-volume samples it is convenient to use the so called Marinelli type container, which has a right-cylindrical shape with a well for the detector in one face. This enables one to measure a large-mass sample in optimal geometry. Extensive measurements of efficiencies in this geometry were reported by Debertin and Ren (57), and computer calculations by by Zikovsky (58).

If a single detector spectrometer is used for very low-level measurements, shielding is needed (cf. Figs. 11 & 12). The background of NaI(Tl) detectors increases with increasing dimensions of the crystals. It depends on the cross sectional area of the crystal (perpendicular to its axis) and does not follow the volume change. Fig. 13 shows a comparison of background count rates (in 0.5 MeV intervals) found for 40×40 mm and 150x100 mm NaI(Tl) crystals. The slope of the curves is the same which means that over the same energy range the background changes in similar proportion for both crystals. In the energy range 3-3.5 MeV, the experimental points deviate from a straight line Here the hard component of cosmic radiation dominates.

The background of an arbitrary NaI(Tl) detector, B_x, can be estimated if we know the background of some reference crystal with the volume V (Ref. 15):

$$B_x = B \cdot (V_x/V)^{0.60}.$$

For minimal background in the region of $E \leq$ MeV, the optimal height-to-diameter ratio of the crystals is about 0.7.

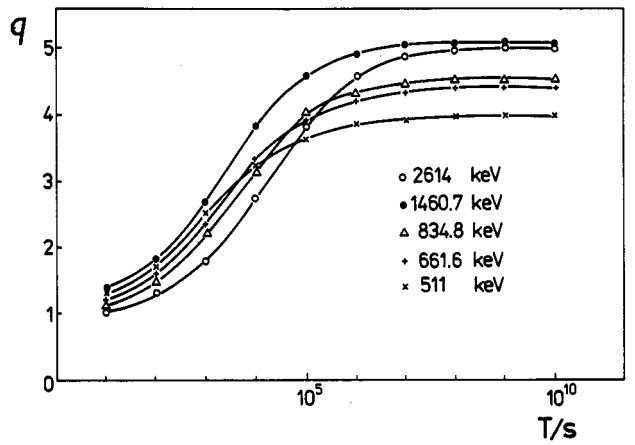

Fig. 11. The dependence of the L_Q values (outside and inside the shield) ratio, q , on the total measurement time for five energies; from Ref. 27.

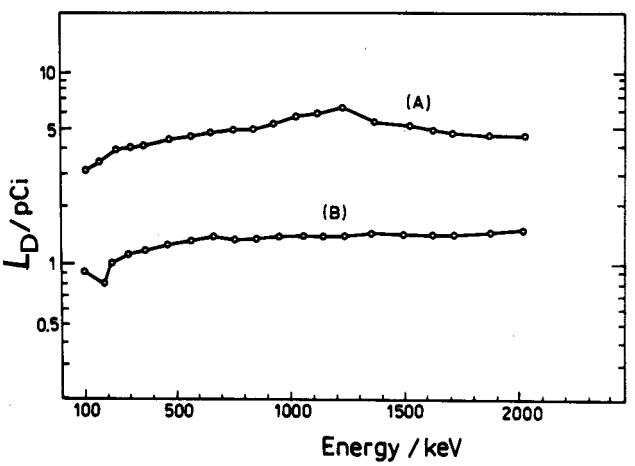

Fig. 12. Comparison of lower detection limits for a Ge detector with a passive (A) and anticoincidence (B) shield. Counting time 1000 min; 1 pCi= 0.037Bq. From Ref. 61.

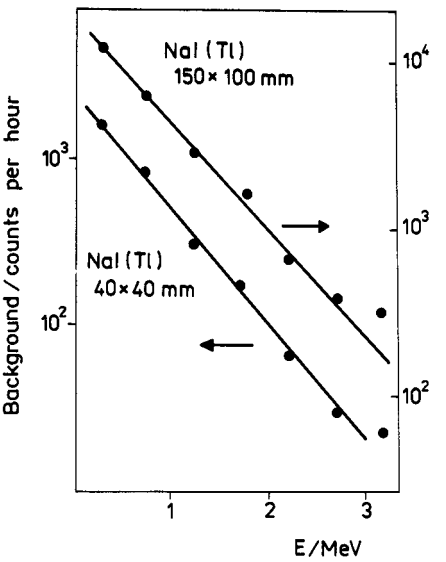

Fig.13. The dependence of the total background of NaI(Tl) crystals on gamma-ray energy (per 0.5 MeV intervals).

The background spectrum of a Ge detector usually contains the gamma-lines of the uranium and thorium series and of ^{40}K (Table 6). Other contributions come from incompletely shielded external gamma rays, from the radiation of contaminants in the shield and detector materials, from airborne ^{222}Rn and its daughter products in the cavities of the shield, from direct muonic events, and from cosmic-ray induced radiation in the detector and the shield.

TABLE 6. Gamma-ray energies usually observed in the Ge detectors background spectra (the most intense peaks)

Energy/keV	Nuclide	Decay series
185.7	^{235}U	^{235}U
186.2	^{226}Ra	^{238}U
209.4	^{228}Ac	^{232}Th
238.6*	^{212}Pb	^{232}Th
241.9	^{214}Pb	^{238}U
270.3	^{228}Ac	^{232}Th
295.2*	^{214}Pb	^{238}U
328.3	^{228}Ac	^{232}Th
338.7	^{228}Ac	^{232}Th
352.0*	^{214}Pb	^{238}U
463.0	^{228}Ac	^{232}Th
511.0*	annihilation peak	
583.1*	^{208}Tl	^{232}Th
609.3*	^{214}Bi	^{238}U
661.6	^{137}Cs	
727.2	^{212}Bi	^{232}Th
768.4	^{214}Bi	^{238}U
794.8	^{228}Ac	^{232}Th
860.4	^{208}Tl	^{232}Th
911.2*	^{228}Ac	^{232}Th
934.1	^{214}Bi	^{238}U
964.4	^{228}Ac	^{232}Th
968.8	^{228}Ac	^{232}Th
1001.2	^{234}Pa	^{238}U
1120.3	^{214}Bi	^{238}U
1238.1	^{214}Bi	^{238}U
1377.7	^{214}Bi	^{238}U
1408.0	^{214}Bi	^{238}U
1460.8*	^{40}K	
1509.2	^{214}Bi	^{238}U
1587.9	^{228}Ac	^{232}Th
1729.6	^{214}Bi	^{238}U
1764.6*	^{214}Bi	^{238}U
1847.4	^{214}Bi	^{238}U
2204.1	^{214}Bi	^{238}U
2614.6*	^{208}Tl	^{232}Th

*most intense peaks.

2.4.3. Anti-Compton spectrometer. "Active" (anticoincidence) shielding is a powerful technique for reducing the detector background. It rejects electronically the spectrometric detector pulse that coincides (within a very short time, a microsecond or so)) with a signal originating in some detectors surrounding the principal spectrometric device. The coincident electronic signals from the active shield and the principal detector are generated by Compton scattered gamma-rays from the shield or detector, and by cosmic ray muons.

An active anticoincidence shield can be devised using GM-tubes, proportional counters, plastic (or liquid) scintilators, NaI(Tl) or BGO crystals. If the anticoincidence system is situated in a passive shield, it is convenient to use NaI(Tl) detectors for space saving reasons. The random distribution of gamma rays from the environment calls for a layer of uniform thickness of the anticoincidence shield surrounding the spectrometric detector. On the other hand, the distribution of cosmic ray muons is largely anisotropic. However, this does not put further constraint on the shape of the anticoincidence shield, since a path length as short as 5 mm within the anticoincidence scintillator is sufficient for the muons to produce detectable signals.

The Compton scattering process in the detector gives rise to a continucus background spectrum (see 2.1, 2.2.) and raises the lower detection limit for the gamma rays with energies in this spectral region. The scattered photons which escaped from the spectrometric detector volume can be detected by a sufficiently large NaI(Tl) or BGO crystal surrounding the detector. NaI(Tl) has a better energy resolution than BGO, but a lower density. As a result, NaI(Tl) is about 2.5 times less efficient than BGO as far as the absorption length is concerned (on the average, for different E_γ's). Due to a lower light output - 10-20% of that from NaI(Tl) - BGO has a higher threshold from the low-energy side, which negatively affects the Compton suppression factor at lower energies. The Ge detector should be placed above the center of the NaI(Tl) crystal for optimal Compton suppression (Fig. 14). For a good Ge detector and large NaI(Tl) crystal (about 30×30 cm), the Compton suppression factor can achieve a value of about 10-12 (for $E_\gamma \leq 1.5$ MeV). Fig. 15 shows the suppression of the Compton continuum in a ^{60}Co spectrum.

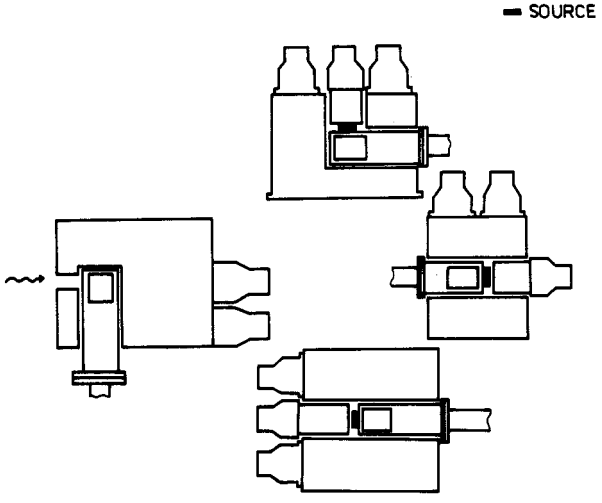

Fig.14. Configurations of anti-Compton spectrometers.

The simplest anti-Compton spectrometer can be realised using a Ge detector and an NaI(Tl) crystal with a well. The influence of this

anticoincidence shield on the background spectrum is demonstrated in Fig.16. A detailed account of the performance of such a device with numerous examples is given by Cooper and Perkins (60). Recent papers of Das (61) deal in detail with the advantage of low level anti-Compton spectrometric measurements.

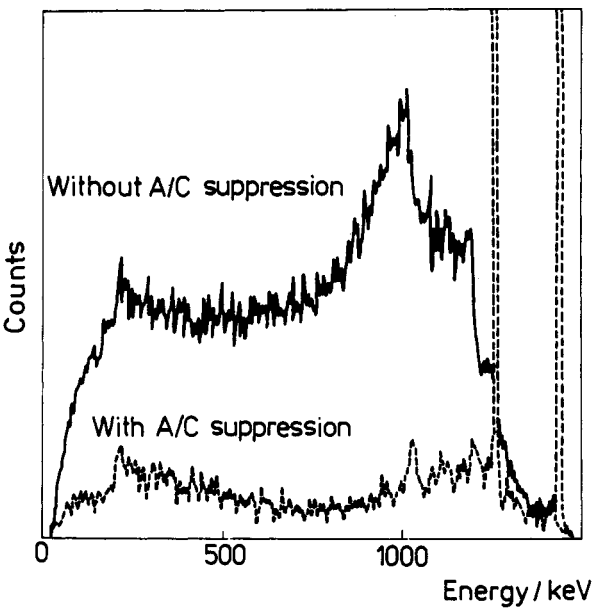

Fig. 15. The ^{60}Co spectrum taken by Ge(Li), with and without a NaI(Tl) anti-Compton shield; from Ref. 62.

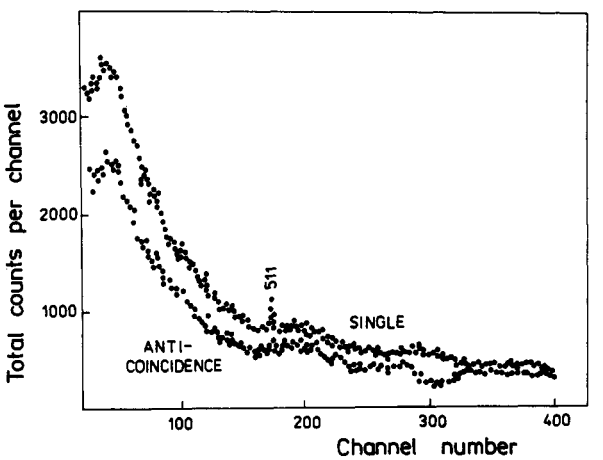

Fig. 16. The Ge(Li) background spectra taken with and without a BGO anticoincident shield; from Ref. 63.

2.4.4. Double coincidence spectrometer. This device is used for measurements of activities emitting coincident gamma rays. The schematic diagram of the electronic circuits of this type of spectrometer is shown in Fig. 17. Usually, two NaI(Tl) crystals, a NaI(Tl) and a Ge detector, or two Ge detectors are used. The Ge - NaI(Tl) spectrometer, which combines the good energy resolution of a Ge detector with the good efficiency of NaI(Tl), is preferable for low-level gamma activities. The advantage of coincidence measurements is demonstrated in Table 7, where the figure of merit values ($F = \varepsilon/\sqrt{B}$) of various spectrometers for registration of annihilation radiation are given.

The count rate of coincidences, N_c, for two coincident gamma quanta (no angular correlation) can be expressed in the following simplified form:

$$N_c = A\varepsilon_1(E_1)\varepsilon_2(E_2)I_{\gamma 1}I_{\gamma 2},$$

where A is the absolute activity of the measured nuclide. This is equivalent to the well-known formula

$$A = N_1N_2/N_c,$$

where N_1 and N_2 are the net count rates in γ_1 and γ_2 FEPs registered in the respective detectors. For the evaluation of an accurate coincidence count rate, the corrections for random coincidences, background, coincidence summing, internal conversion probability, and coincidence efficiency must be considered. The number of random coincidences, N_A, can be estimated from the expression

$$N_A = 2\tau N_1.N_2,$$

where τ is the coincidence resolving time.

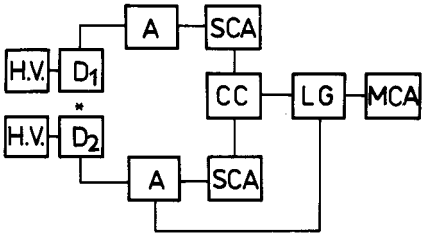

Fig.17. Schematic diagram of electronic circuits of double coincidence spectrometer. SCA - single channel analyser, CC - coincidence circuit, LG - linear gate, MCA - multi-channel analyser, H.V. - high voltage, D - detector, A - amplifier.

TABLE 7. Comparison of various types of spectrometers for measuring $\gamma^{\pm}$; from Ref. 27.

Spectrometer	Background /cps	ε/%	F
single Ge(Li); 70 cm^3	0.046	1.43	6.67
single NaI(Tl); 100×100 mm	7.1	8.86	3.32
Ge(Li) - NaI(Tl)	0.0045	0.68	10.14

2.4.5. Triple coincidence spectrometer. This type of spectrometer is typically used as a pair spectrometer for the simultaneous registration of the annihilation and de-excitation radiations of β^+ active nuclides. Three NaI(Tl) crystals or two NaI(Tl) crystals and one Ge crystal can be used in this spectrometer configuration. Often a large NaI(Tl) crystal split into two optically isolated sections is used, which can also be employed in the anti-Compton spectrometer. The triple coincidence scintillation spectrometer (Ref. 17) with passive and active shields, was used for measurement of ^{22}Na, ^{26}Al and ^{60}Co

concentrations in meteorite samples (≈ 160 g). It increased the sensitivity for ^{22}Na in the presence of higher ^{26}Al and ^{60}Co activities as compared with the double coincidence spectrometer (see Ref. 64).

The triple coincidence spectrometer, though displaying a very good selectivity and a very low background, has a low efficiency.

2.4.6. Sum-coincidence spectrometer. This spectrometer operates on the basis of coincidence summing of cascade (or annihilation) gamma rays. Setting the energy window of the SCA in the summing part of the spectrometer on the sum of cascade gamma quanta permits recording in the MCA only full energy absorption peaks. The purity and resolution of such spectra are better and processing is also simpler. Table 8 shows a comparison of the performance characteristics of various spectrometers. The sum-coincidence spectrometer is convenient mainly for samples which contain many radionuclides.

TABLE 8. Minimum measurable activity (see sect.2.4.1.) of ^{22}Na (E_γ = 1.275 MeV) for various NaI(Tl) scintillation spectrometers (meas. time 24 h); from Ref. 65.

Spectrometer	ε/%	Background/cps	L_Q/(Bq/kg) at σ=10%
single NaI(Tl)	5.45	0.60	5.7
double coincidence	0.76	0.019	3.7
sum-coincidence	0.84	0.017	3.4

2.4.7. Beta-gamma coincidence spectrometer. In this spectrometer a beta detector (a GM, proportional, or a Si/Au detector) is usually combined with a NaI(Tl) or Ge crystal. The beta-detector (usually of a disk shape) can have a high efficiency (large area), low background and low sensitivity to gamma radiation. The thickness of samples is limited by absorption of beta particles. The 4π or $2\times2\pi$ geometry is used for measurement.

Using the beta detector in the triple coincidence spectrometer we obtain the β-γ-γ spectrometer (Ref. 66), which can be used for the investigation of radionuclides emitting two cascade gamma rays after beta decay, or for positron activities. The selectivity of this spectrometer is similar to that of a double-coincidence spectrometer, but its background is about two orders of magnitude smaller; therefore, its minimal measurable activity is substantially lower. This type of spectrometer is the best choice for analysing thin samples.

TABLE 9. Figure of merit for various scintillation spectrometers (with 150x150 mm NaI(Tl) crystals)

Spectrometer	Background/cps	ε/%	*F*
single NaI(Tl)	1.2	20.2	18.4
NaI(Tl) - NaI(Tl)	0.008	9.9	110
two-parameter	0.005	11.9	168

2.4.8. Two-parameter spectrometer. This type of spectrometer can be constructed, e.g., from CAMAC modules and a computer (Ref. 67). Signals from two detectors create three-dimensional spectra which contain both coincidence and non-coincidence peaks. The background is reduced, and three-dimensional spectra enable a better identification of peaks to be made. As it follows from Table 9, this spectrometer is the best among scintillation spectrometers for the measurement of annihilation radiation.

2.5. Conclusion

For very low-level gamma-spectrometry, it is most convenient to use Ge(Li) or HPGe detectors with their very good energy resolution although their detection efficiency rapidly decreases when a point source is substituted by a large volume source. Therefore sometimes, if large-volume samples containing only radionuclides with a simple decay scheme need to be analyzed, it is better to use large NaI(Tl) crystals. Passive and active (optional) shielding of the spectrometer are necessary to reduce the background when very low-level activity samples are to be processed. Coincidence arrangements may permit a substantial increase in the selectivity of the spectrometer.

For very small samples it is more convenient to use beta-gamma coincidence spectrometers. This type of spectrometer has been applied succesfully for the measurement of cosmogenic radionuclides in lunar samples with a mass of about 50 mg (Ref. 65).

Low-level gamma-spectrometry needs long measurement times; therefore, long-term stability of the equipment is required. For example (see Ref. 68),temperature changes of about 2 °C during 24 hours may shift the spectrum of the Ge(Li) spectrometer by about one FWHM (the energy resolution was 2 keV at 1.33 MeV). By using an electronic spectrum stabilizer these shifts can be reduced substantially.

In conclusion, we can state that for most applications a large-volume HPGe spectrometer with relative efficiency of about 50% is the best choice, especially when multicomponent samples are to analysed. A higher sensitivity can be reached using more sophisticated coincidence-anticoincidence systems usually combined with NaI(Tl) detectors.

3. LOW-LEVEL ALPHA-PARTICLE SPECTROMETRY

3.1. Characteristics of alpha-particle spectra

Natural radionuclides emit alpha particles within an energy interval of 2 to 9 MeV; in products of nuclear reactions this span is up to ≈ 12 MeV (^{212m}Po; E_α=11.65 MeV, $T_{1/2}$=45 s). There are several compilations of alpha particle energies and intensities; see, e.g., Refs. 69 & 70.

Mere low-level counting is seldom required; in general, high sensitivity spectrometric measurements are needed. An instrumental alpha spectrum consists, in principle, only of the full energy peaks; see Fig. 18. Even Z - even A nuclides have usually only one intense line; odd-even, even-odd, and odd-odd ones may have several lines of comparable intensity. Tailing of an otherwise ideal peak may be caused by a finite (and the more, uneven) thickness of the sample layer as the range of alpha particles is 10 mg/cm^2 or so. The ranges and stopping powers as functions of E_α and of Z of the stopping material are tabulated, e.g., in Refs. 71 & 72; some of the data are displayed in Fig. 19a,b.

The background of alpha-spectrometric systems is usually very low and smooth. It originates from radioactive impurities in the construction materials (see Ref. 73) and from cosmic rays.

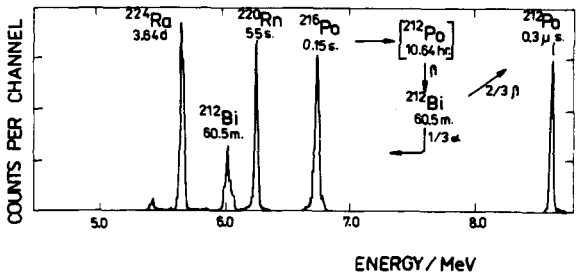

Fig.18. Alpha spectrum of the ^{224}Ra series taken by a surface barrier detector with 14 keV resolution; from Ref. 75.

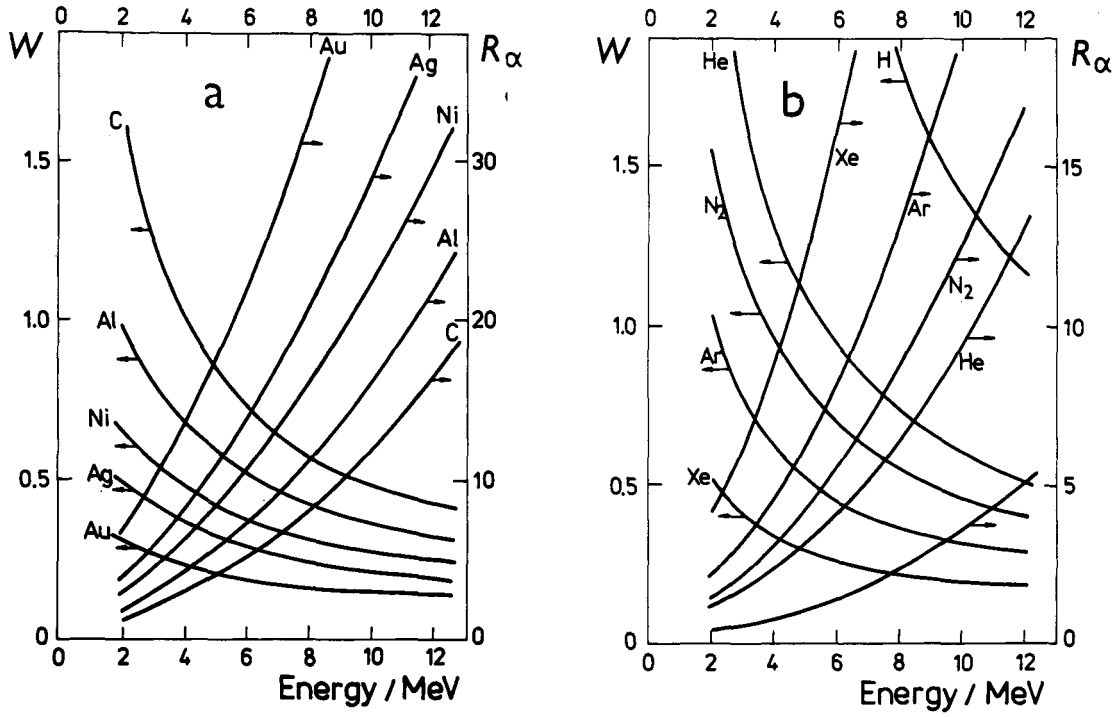

Fig. 19. Calculated values of stopping powers, W, and ranges, R_α, of alpha particles in some solids (a) and gases (b) as functions of E_α; from Ref. 71.

3.2. Alpha spectrometric detectors

All types of detectors mentioned below have to be calibrated using energy standards. The dependence of the pulse height on the particle energy is usually almost linear. The detection efficiencies for thin samples are independent of energy.

Modern semiconductor surface barrier detectors (Si/Au and others) have energy resolution (FWHM) as low as 15 to 20 keV, i.e., some 0.3% for a 6 MeV line. The efficiency is nearly 100% for the particles which hit

the detector but, as they are emitted isotropically, for optimal source-to-detector geometrical arrangement the actual efficiency is some 80% of 2π.

Small (100 cm^2 in cross section) "gridded (Frisch grid)" ionization chambers have a somewhat poorer resolution than the afore-mentioned semiconductor detectors, but a better efficiency - almost 100% of 2π - because the sample is placed into the sensitive volume. These values hold for samples with surface density less than about 50 $\mu g/cm^2$ (The layer should be homogeneously thin in the sense that any single particulate of a powdered sample should be smaller than the average sample thickness.)

As the surface barrier detectors are at present available in sizes of aereas not larger than a few tens of cm^2, the only solution for samples with a mass above 10 mg is to increase the size of ionization chambers. Of course, somewhat thicker samples may be analyzed provided that the spectrum is so "clean" that the loss of resolution does not affect the selectivity. In any case, 1 to 2 mg/cm^2 seems to be the limiting thickness for "spectrometric" measurements. Finite thickness causes tailing of the peaks and shifts the average energy of the recorded events towards lower energies (Ref. 75). If the energy of alpha particles is E_o, their full range in the sample material is R, and the thickness of the layer is d, then the shape of the observed peak is given by

$$N(E)dE \sim (E_o^{3/2} - E^{3/2})EdE,$$

where E is the measured particle energy. Then the average energy in the observed peak is given by

$$E_{av} = E_o[R/(6d+R)]^{2/3}.$$

For an "infinitely" thick source ($d \geq R$), we obtain $E_{av} = 0.274E_o$.

Unfortunately, for fundamental reasons (large electrical capacity), very large ionization chambers have increasingly poorer resolution compared to the small ones.

Two other techniques for low-level alpha measurements are of lesser use. The first one is liquid scintillation alpha-spectrometric counting (Ref. 10). Recently, by "on-line" computer analysis of the shape of the electronic signal, it has proved possible to clearly differentiate between alpha and beta particles of the same energy . This is very important from the point of view of reducing the background (see, e.g.,Ref.76) as the maximum range of beta particles in the scintillator is much smaller than the size of the sensitive volume and the particles deposit their full energy. The latter is not the case in the ionization chambers and semiconductor detectors (see below), where only a fraction of beta energy is deposited. The energy resolution (FWHM) of liquid scintillation spectrometers is $\geq$ 5%. As the sample has to be dissolved in the scintillation "cocktail", there are limitations as to its permissible chemical nature and amount. Still this kind of detector can be very useful, for example, for measurements of plutonium or radon.

The second technique is based on the fact that heavily ionizing particles, such as alpha particles or fission fragments, produce latent tracks while stopping in dielectrics (see also Chapter 4). The tracks are quite stable at room temperature, and by chemical etching with proper agents they can be enlarged to several micrometers in length and diameter. Then they can be seen and, hence, sought for by optical microscopy. Alpha particles can be registered only by the most sensitive of these "solid state track detectors" (SSTD), CR-39 plastic

measuring the diameter and other parameters of the etched tracks. The SSTD technique is quite efficient and essentially free of background, except for some etchable surface defects which might imitate the true alpha particle tracks (they occur in variable concentration).

The track detectors do not register beta or gamma rays for fundamental reasons - the etchable track is formed only if the particle stopping power of exceeds some (material dependent) threshold. The energy resolution of SSTD seems to be generally poor, although some authors (Ref. 77) claim achieving 35 keV FWHM with CR-39. Results are obtained only after exposure and etching, not in real time. Scanning large areas of detectors is tedious. Each batch of the SSTD material needs to be calibrated. Similar problems also characterize the classical "nuclear emulsion technique". For these reasons, the two methods are seldom used for low-level alpha spectrometry.

3.3. Performance of large ionization chambers

The measures necessary to reduce the background in alpha spectrometry are mostly the same as those involved in gamma counting. Fortunately, ionization chambers (as well as semiconductor detectors) have a weak response to energetic electrons (beta-particles, Compton and photoelectrons produced by gamma radiation) in the sense that the energy of these beta particles is underestimated by the device. The reason is that the range of electrons is longer by about two orders of magnitude than that of alpha particles with similar energy, while it is the alpha particles which determine the necessary linear size of the chamber. This is why the background of the chamber is significant strongly and strongly increases below effective 2 MeV. It does not cause much trouble in most measurements, although excessive beta activity in the sample and irradiation of the chamber by external gamma rays is by no means desirable. Because of the small ranges of alpha-particles, only materials comprising the surface of the sensitive volume of the chamber have to be free of U or Th contaminants. Omnipresent airborne radon brings a lot of problems because radon may enter the chamber during changing of the samples, and also the sample in the course of its preparation and storage is liable to contamination by radon and its decay products. Sometimes the only solution may be to start measurements as late as two days after charging the chamber to let ^{212}Pb ($t_{1/2}$=10.6 h) decay. As to the contamination of samples with naturally occurring series, it should be kept in mind that because of different chemistry, the progenies in the well-known ^{238}U, ^{235}U and ^{232}Th families may not necessarily be in secular equilibrium. Thus radium may be present while U and Th are completely absent, or ionium (^{230}Th from the ^{238}U series) may occur without uranium.

With any high-efficiency alpha spectrometer there is an interesting possibility of recognizing decay events from members of radioactivity series which occasionally might interfere with different activities sought for (Ref. 78). One measures the time of detection of each alpha particle. If two successive particles have the energies of a known parent - daughter pair and the time interval is consistent with the half-life of the daughter, the two counts are rejected. Examples of such pairs - $^{224}Pa/^{220}Rn$, $^{220}Rn/^{216}Po$, etc.- can be seen in Fig. 19. On the other hand, even in complex spectra of mixtures of natural radioactive series, through identifying "delayed coincidences" of decay events of a relatively short lived nuclide with the decays of its progenitor it is possible to determine the absolute activity of the progenitor(s)(Ref. 79)

It should be remembered that a number of man-made alpha active nuclides which otherwise would not exist in nature in detectable amounts or

concentrations have been and are being produced in weapon and power technologies. These are quite long-lived isotopes of Po and of elements from Pa to Cm or even Cf. Since they are used in portable neutron sources, pacemakers, smoke detectors, for cancer treatment, and other applications, these isotopes can unexpectedly emerge anywhere in the environment.

There are some rather curious examples of these problems. In some batches of commercial hydrofluoric acid there were found minute activities of almost "pure" (in the sense of alpha spectrum) ^{234}U. The acid was evidently produced at a diffusion plant by hydrolysis of enriched UF_6. Some commercial lanthanide radiotracers are isolated from fission products, and very sensitive measurements may reveal alpha-active isotopes of Am and Cm in the preparations.

Cosmic rays must produce background counts in the energy range of interest in alpha spectrometric measurements, especially in the huge volume (see below) of the "large" ionization chamber, although most of them fall below the equivalent of 2 MeV alphas. No systematic data have been found in the literature.

Optimal geometrical and electrical parameters of large ionization chambers are the subject of Ref. 80. Based on this paper, a cylindrical chamber was built at the Joint Institute for Nuclear Research (JINR), Dubna, Russia (Ref. 81). The cathode has a diameter of 220 mm with the sample area being up to 4500 cm^2. It is kept at -2600 V vs. ground. The grid of 110 mm diameter (99.4% transparency) is at -2300 V. The grounded collection electrode has a diameter of 8.6 mm, the output capacity is 15 pF. With the working gas 94% Ar + 6% CH_4 at 1.5 atm, the resolution measured for 5.8 MeV alphas was 55 keV. An even larger chamber of similar construction with a sample area of 2 m^2 was built at Comenius University, Bratislava, Czechoslovakia (Ref. 75). Its resolution is 120 keV for ≈ 5 MeV alphas. A gridless chamber of approximately the same size and characteristics was built at the University of Uppsala, Sweden (Ref. 82). Its background is 0.8 cpm in the range 4.0 to 5.0 MeV.

4. LOW LEVEL SPONTANEOUS FISSION COUNTING

4.1. Spontaneous fission activities

There are dozens of quite long-lived (several days and longer), man-made transuranium nuclides with an appreciable spontaneous fission (SF) branching and many more short-lived ones; for their radioactive properties, see Refs. 83 & 84. At the same time, the only primordial nuclide showing a detectable SF activity is ^{238}U with a partial SF half-life of 8.2×10^{15} years. So its specific activity is about 7 SF events per kg per second (alpha/SF activity ratio is 1.83×10^6). For some 20 years there have been conducted unsuccessful searches for the so-called superheavy elements, SHE, of primordial origin with Z values supposedly lying in the region of 110 to 114 or so, which were expected to experience SF. These studies stimulated the development of some of the below-mentioned SF counting equipment of unique sensitivity.

4.2. Properties of fission fragments

All the measurable characteristics of the fission process, such as the energy of single fragments, the total kinetic energy of the two

fragments, the number and energy of prompt gamma rays, and the number of prompt neutrons, ν, show a very broad distribution with a width comparable to the whole range of the actual values of these parameters for known SF-nuclides. This dispersion originates primarily from the very broad (mostly double-humped) mass yield distribution of fission fragments, which is projected onto fragment energies (see Fig. 20) and the other parameters due to the laws of conservation of momentum and energy. For these reasons, especially in low level counting, different nuclides cannot be distinguished from each other, except the short-lived ones, whose half-lives can be measured directly.

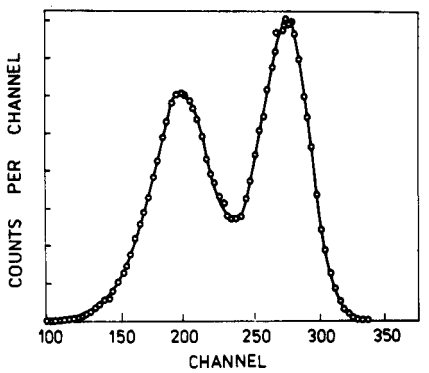

Fig. 20. Pulse-height spectrum of ^{252}Cf fission fragments taken by a semiconductor detector. Peak energies are 80 and 105 MeV.

The most probable total kinetic energy (TKE) of fission fragments is fit by (see Ref. 85)

$$TKE = 0.119\ Z^2/A^{1/3} + (7.3 \pm 1.5)\ MeV,$$

where Z and A are the atomic and mass numbers of the fissioning nucleus. The kinetic energy of a single fission fragment exceeds 50 MeV and can be as high as 120 MeV. This holds both for spontaneous and induced fission. The ranges of fission fragments are then about 3 times shorter than those of alpha particles (see Table 10 and cf. Fig.19a).

TABLE 10. Mean linear ranges of fission fragments in some gases and mass ranges in various metals; data for induced fission of ^{238}U.

Material	Fragments light	heavy	Material	Fragments light	heavy
	range/(mm at STP)			range/(mg/cm^2)	
H_2	21.1	17.7	Al	4.17	3.22
He	28	23	Ni	5.5	4.3
Ar	25	19	Ag	7.3	5.5
Xe	23	18	Au	10.7	7.8

The charge of a moving fission fragment depends on its Z, A, and velocity and on Z of the stopping medium. It has been found empirically that the residual range can be described by the relation

where E is the energy in MeV, c is 0.193 and 0.183 mg Al/cm^2 for the average light and heavy fragments, respectively, or 0.143 mg air/cm^2 for all the fragments (Ref. 86). Generally, the problems with the finite thickness of a sample layer are analogous to those in alpha measurements (cf. 3.2.).

4.3. Detection of fission fragments

As the alpha-particles, fission fragments also may be detected by semiconductor surface barrier detectors and ionization chambers. Proportional counters can be used too, but one should remember that the amplitude of pulses from fission fragments in proportional counters is much smaller than it would follow from calibration with alpha particles (saturation effects). In using the above types of ionization detectors, there are usually no problems with the alpha, beta or gamma activities present in the sample because they have much smaller particle energy than do fission fragments.

SF activities as contaminants in contruction materials must be exceptionally rare. Nevertheless, caution must be exercised as ^{252}Cf ($t_{1/2}$ = 2.6 y; alpha/SF ≈ 30) is at present used for some applications and in nuclear physical experiments. Contamination of surfaces with this nuclide might not be improbable, the more so because open sources of Cf experience self-sputtering due to the recoil from fission fragments.

Pulses produced in the sensitive volume by ionizing cosmic radiation are relatively small and cannot be compared with those from fission fragments. In any case, active anticoincidence shielding is feasible. The experimenter must take into account the possible background from cosmic ray induced fission of heavy elements (e.g. Pb), if present in the sample. These give rise to an apparent SF half-life of 10^{20} to 10^{21} years for lead at the sea level (Ref. 87).

A highly sensitive proportional counter was developed in JINR, Dubna; see Fig. 21 (Refs. 87 & 88). It is a 2000 mm x 260 mm i.d. cylinder with the sample to be measured painted (up to 3 mg/cm^2) onto two semicylindrical cathodes. Their total area is 1.4 m^2 so that the mass of the sample may be as large as 50 g. The anode is a 50 μm nichrome wire at 1200 V, the volume is filled with methane at a pressure of 50 mmHg. The efficiency of detecting a SF event is about 60%. The apparent SF half- life for electromagnetically enriched ^{208}Pb measured with this device under a 2 m thick concrete shielding was 4×10^{21} y, the background of the counter was less than one count per month. Six such counters were operated simultaneously in searching for SHE (Ref. 87).

4.4. Detectors of prompt neutrons

In contrast to the above detectors for ionizing fission fragments, in prompt neutron detectors a "burst" of prompt, fast (1 to 2 MeV) neutrons accompanying a SF event is registered. This permits measurements of voluminous and/or large mass samples. The neutrons are emitted from the "hot" fission fragments within some 10^{-14} s, their average number ranges from 2 to 4 (again, the dispersion is large), being a roughly linear function of Z^2/A of the fissioning nuclide. To be efficiently registered, the neutrons must be first slowed down. Then they diffuse and are with certain probability captured by the counting medium. So the fingerprint of a fission event is the registration of

two or more neutrons within a time interval of several average neutron lifetimes in the moderator plus detector system, usually some 50 μs. Registration of a single neutron cannot be used for detecting SF as the background is high.

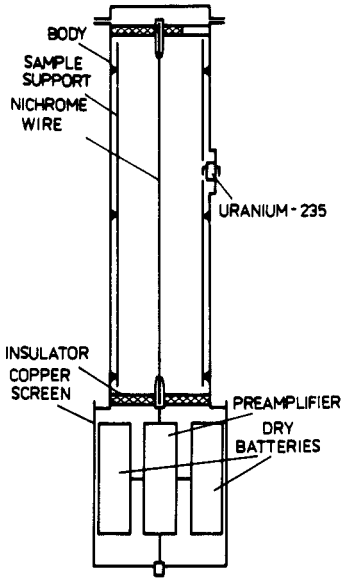

Fig. 21. Large proportional SF-counter at JINR, Dubna. The ^{235}U target, when exposed to a neutron source serves for calibration; from Ref. 89.

There are several options for thermalizing and detecting the neutrons. For example, in a tank of 50 to 100 cm diameter filled with a liquid scintillator loaded with some Gd salt, the slow neutrons are captured by Gd nuclei; cf. Fig.22a (Ref. 90). The total energy of the neutron capture gamma rays is large, some 7 MeV, and a large portion of it is absorbed in the scintillator in each capture event. Then by setting the appropriate energy window for the sum of pulses from the PMTs viewing the scintillator, one can detect fission events. This is the least expensive but not the best equipment for detecting rare SF events. The single neutron efficiency is very good, some 85%, but the background is high due to random coincidences of gamma rays in the huge sensitive volume.

A better set-up consists of a solid moderator with an array of BF_3- or ^3He filled proportional counters in its volume. The dedicated installation in the JINR Flerov Laboratory of Nuclear Reactions (Refs. 89 & 91) consists of a 700 mm long, 550 mm i.d. plexiglass cylinder with a through channel of 160 mm in diameter in which the sample to be measured is placed. Fifty-six counters are arranged around the channel, each one 500 mm long and 32 mm in diameter. They are filled with ^3He (+ 1% CO_2) at a pressure of 7 atm. Each counter, together with a preamplifier and a high voltage supply (1000 V), constitutes a separate module. The single neutron detection efficiency is 48% for the center of the sample hole and the detection efficiency for the SF events of ^{252}Cf (ν = 3.73) is 58% if measured as multiple ($\geq$ 2) neutron coincidences within 60 μs. The equipment was placed at a depth of 1100 mm w.e. in a salt mine (Solotwino), where it showed less than one multiple neutron coincidence per month. A similar installation at ORNL USA with somewhat poorer characteristics, was described in Ref. 92.

In the upgraded JINR counter (Ref. 89), the neutron detection is triggered by the registration of the burst of prompt gamma rays (in average, 5 to 7 gamma rays are emitted within 10^{-8} s) rather than by the first prompt neutron detected. This is done by using an array of ten BGO scintillation detectors placed in the 160 mm central hole; they surround a sample which now can be of more limited mass(Fig. 22c).

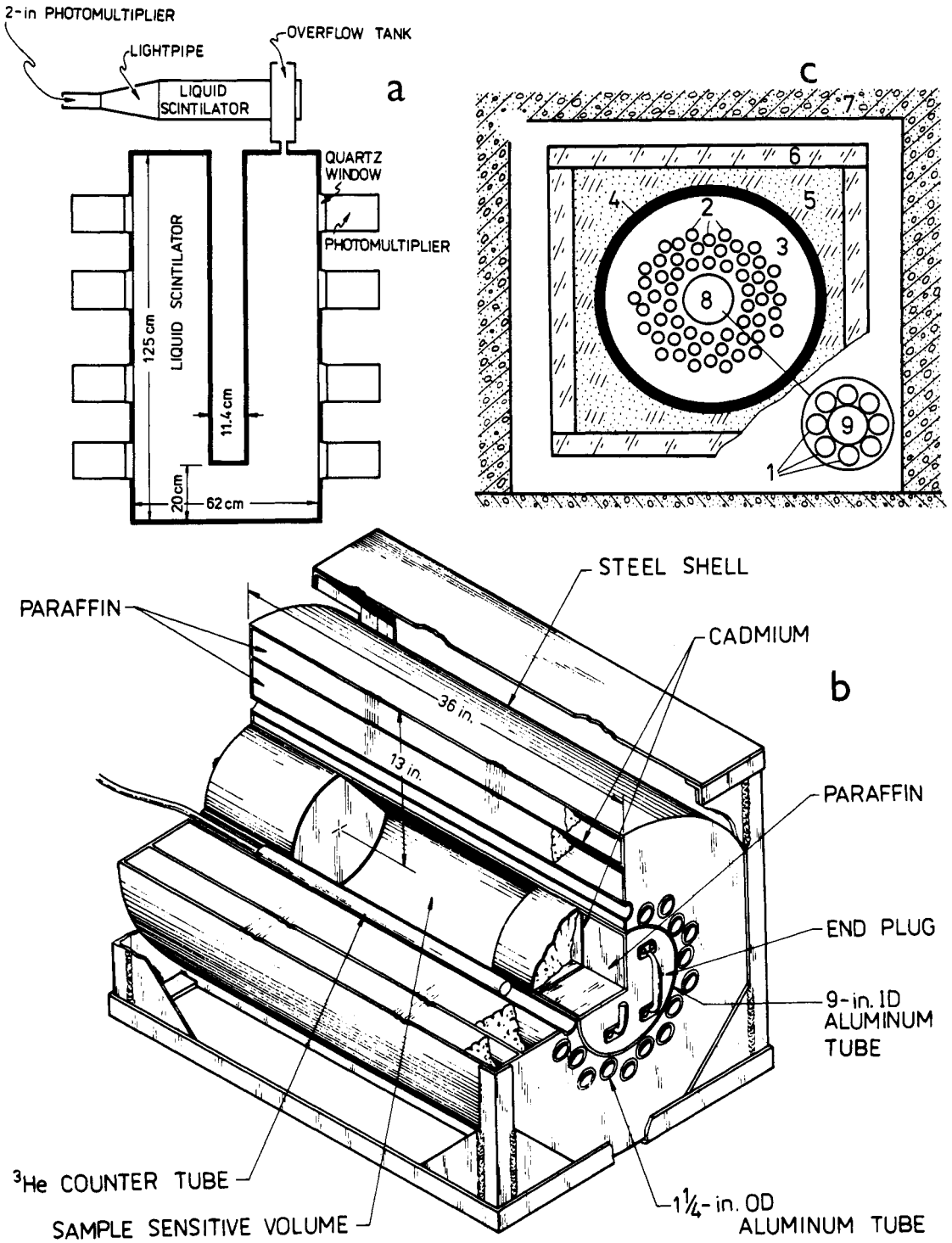

Fig. 22. Neutron multiplicity counters. a - Gd-loaded liquid scintillator at LBL, Berkeley (Ref. 90); b - moderator + ^{3}He counters at ORNL, Oak Ridge (Ref. 92).; c - moderator + ^{3}He counters + BGO trigger at JINR, Dubna (Ref. 89): 1 - BGO detectors, 2 - ^{3}He counters, 3 - moderator, 4 - Cd, 5 - polyethylene, 6 - plastic scintillator, 7 - concrete, 8 - sensitive volume, 9 - sample volume.

Now the fingerprint of a SF event is the multiple coincidence of gamma rays within < 1 μs, plus one or more neutrons within 50 μs. The efficiency of detecting the SF of ^{252}Cf is as high as 80%.

Very recently Barton *et al.* (93) reported on a novel neutron multiplicity detector at the University of London, UK. Efficient neutron counters were constructed using layers of LiF + ZnS mixture, the scintillation light being transmitted to photomultipliers by wavelength shifting light guides; polypropylene served as the moderator. An array of these countres had a detection efficiency of 37±2% for fission neutrons, its measured background rate for threefold neutron events a a depth of 60 m w.e was about one event in two days.

4.5. Spinner (a "bubble chamber")

A very specific technique for low-level SF counting was developed using the principles of a bubble chamber (Ref. 94). An (alcoholic) solution of the sample is loaded into a rapidly rotating glass cylinder with long glass arms; see Fig.23. The centrifugal force produces a negative pressure in the liquid and when a fission events occurs the metastable state is destroyed by forming a bubble. The bubble causes a rise in the level of the liquid in the arm and this can be recorded, e.g., photometrically. The device is insensitive to alpha, beta or gamma radiation; it has a very low background and a 100% counting efficiency. As many as several tens of grams were measured with vessels of 75 cm^3 volume.

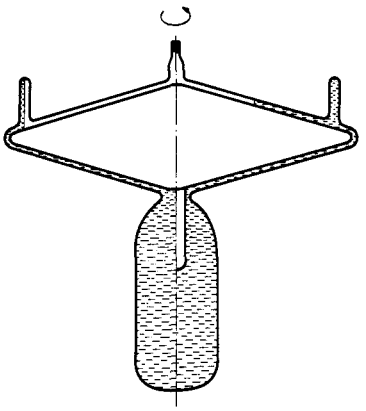

Fig.23. Spinner detector; from Ref. 94.
The left side is the metastable state,
the right side is the broken state.

4.6. Solid state track detectors

A variety of dielectrics may serve as SSTD for SF measurements (cf. 3.2.) as the fission fragments are heavily ionizing. The most popular ones, characterized by good selectivity and low background, are CR-39 plastic, polyethyleneterephthalate foils, glass and synthetic mica (for use at higher temperatures). Detection of fission fragments by SSTD is reviewed in Refs. 95 & 96. The detectors do not permit measurements in real time; the result is obtained only after finishing the exposure and etching. They have been used for very low-level counting of SF in massive (up to some 100 g) samples but the scanning of large areas is a very time-consuming and tedious procedure. Very similar problems are encountered with nuclear (photo)emulsions.

5. DEEP UNDERGROUND FACILITIES

M. Sakanoue, Kanazawa University, Japan

In last years, several deep underground facilities have been built designed mostly for experimental studies to test the theories of elementary particle physics, cosmophysics and nuclear physics (see Ref. 97 for the present status). But, in any case, the underground caves can be used (and some already are) to house very low-level counting devices which were described in previous chapters. With this in mind, these facilities are surveyed as for their basic features and experimental programs.

The primary purposes of the facilities, some of which are listed in Table 11 may be summarized as follows:

measurement of the proton decay constant (p);
search for magnetic monopole (mm);
measurement of the flux of the solar and galactic neutrino (ν);
studies of muon flux variations - (μ);
search for high-energy neutrino sources (νE);
measurement of double-beta decay lifetimes ($\beta\beta$);
determination of extremely low level radioactivity under very low-background conditions (LLR).

The last topic includes measurement of self-background of various radiation detectors or dosimeters, studies of the origin of the background at the facility, and other studies relating to radiochemistry and radiobiology.

TABLE 11. Underground facilities for measurements of very low levels of radioactivity and/or radiation.

	Approx.depth/ m w.e.	Location; "project"	Country	Expt. program
A.	8400 + smaller	Kolar Gold Field, South Deccan Plateau; "KGF"	India	p
* B.	5000	Mont Blanc, Alps	Italy	p,ν
C.	4400	Frejus tunnel, Alps;"FREJUS"	France	p,ν
D.	4400	Homestake mine, South Dakota	USA	ν
* E.	4000	Gran Sasso, Abruzzi	Italy	ν,p,$\beta\beta$,mm
* F.	4000+smaller	Baksan, Caucasus	Russia	ν,$\beta\beta$
G.	3000	Gotthard-Strassen tunnel,Alps	Switzerland	
H.	2700	Kamioka mine, Gifu Prefecture	Japan	p,ν
I.	1800	Soudan iron mine, Minnessota	USA	p,ν
J.	1570	rock salt mine, Cleveland, Ohio; "IMB"	USA	p,ν
K.	1000	salt mine, Solotwino,	Ukraine	$\beta\beta$
L.	700	Miboro dam site, Gifu Prefecture	Japan	LLR
* M.	390	Mining Academy, Freiburg	Germany	LLR
N.	300	Ooya stony cave, Tochigi Prefecture; "COSMUD"	Japan	
O.	180	Nokogiriyama, Chiba Prefecture	Japan	
P.	180	Saberio	Georgia	LLR
* R.	125	Rossendorf, Saxony	Germany	LLR
S.	70	Phys.Inst.University of Bern	Switzerland	LLR

* already mentioned in section 2.3.3.

In Fig. 24 a profile of the Kolar gold field is shown, with the location where proton decay measurements are done. Attenuation of the muon flux with depth is shown in Fig. 25 according to the data obtained at this site.

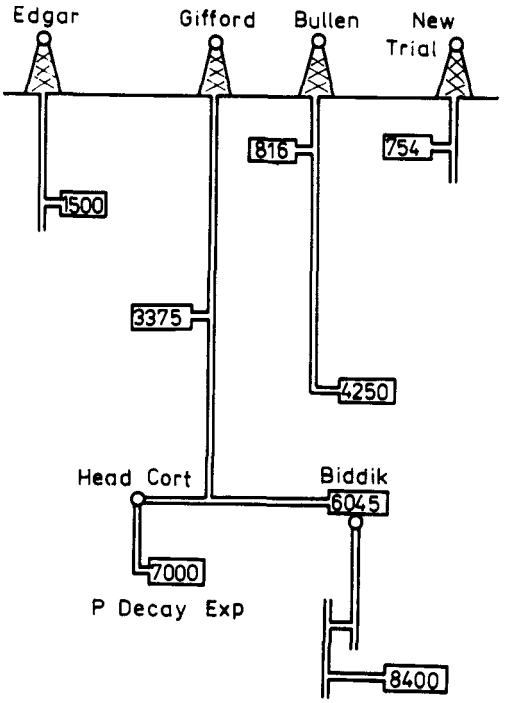

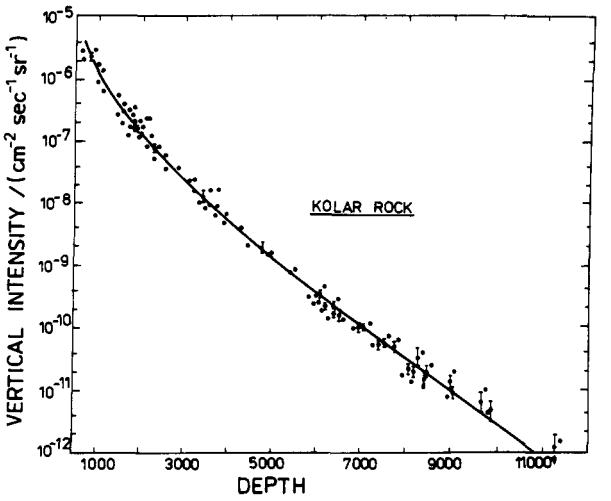

Fig. 24. Depth profile of KGF. Depths are given in m w.e..The The ground elevation is 900 m.

Fig. 25. Attenuation of muons with depth

Neutrinos, especially the high-energy ones, interfere with proton decay studies. On the other hand, neutrino flux measurements can be done using similar facilities, as neutrinos of various origins regularly impinge upon the earth. In 1987, the proton decay facilities "H" and "D" incidentally caught Čerenkov signals due to a neutrino burst from the Supernova SN1987a.

Solar neutrinos are produced mainly by the nuclear fusion process and have a rather low energy. For such sophisticated investigations, it is very important to reduce the background due to the presence of various natural radionuclides, e.g., ^{238}U and ^{226}Ra in the detector system (water tank). The contribution of beta particles from ^{214}Bi, descending from the airborne radon and trapped in water, is the most serious problem.

Solar neutrinos can be detected indirectly, by recording the products of neutrino-induced reactions of the inverse beta decay type. Some of them proceed with cross-sections of the order of 10^{-42} cm^2 and have different threshold energies.The nuclei produced must be radiochemically isolated and measured with high resolution against an extremely low background. For example, an experiment designed to extract ^{37}Ar from 619 tons of perchloroethylene liquid has been performed at facility "D". The contribution of cosmic-ray muons to the production of ^{37}Ar is examined by using a ^{39}K target in which ^{37}Ar is

produced by muons with a higher cross-section (42 mb) than that in ^{37}Cl (0.027 mb). A similar experiment is planned at facility "F".

Experiments using gallium targets are planned at the facilities "D", "E" and "F". In this case, extraction of Ge in the form of $GeCl_4$ will be made from about 50 tons of Ga as $GaCl_3$, and beta particles of ^{71}Ge will be counted after synthesizing GeH_4 from $GeCl_4$.

For ^{115}In as a target, direct measurements of two gamma rays of 116 and 498 keV should be done with an extremely low background, while for ^{205}Tl a large amount of thallium minerals without lead contamination, e.g., $TlAsS_2$ (lorandite) is expected to provide high enough sensitivity to detect ^{205}Pb produced at very low levels.

The phenomenon of neutrinoless double beta decay is related to the problem of violation of the leptonic number and of the neutrino mass. The following nuclides are the candidates for double beta decay studies; their expected half-lives are not shorter than the indicated values:

^{48}Ca	10^{19}-10^{21} y
^{76}Ge	10^{22} y
^{130}Te	10^{21} y
^{150}Nd	10^{20} y

To obtain accurate results for such low-level radioactivity, an extremely low-background counting system placed underground is indispensable. At facility "H", the double beta decay of ^{76}Ge is sought for. The search consists in looking for the 2.05 MeV "gamma rays" (actually the sum of two beta particles) in large volume Ge detectors. As contributors to the background, the alpha particles from the radon gas adsorbed on the surfaces of the Ge crystal and other parts have been identified. Neutron- and proton-induced activities of the surrounding rocks also interfere with such measurements. The background also derives from cosmic-ray induced activities in the detector material, e.g., from 288-day ^{68}Ge in equilibrium with its ^{68}Ga daughter which emits hard gammas. To suppress them, some researchers manufacture the crystals from materials (starting with the raw ones) which were kept above ground for as short a time as possible. The fabrication of the crystals from electromagnetically enriched ^{76}Ge (natural abundance, 7.8%) to increase the sensitivity of measurements has also been reported.

Acknowledgement - The authors would like to thank Dr. S.R. Joshi and Prof J.W. Lorimer for most valuable comments.

6. INSTITUTIONS AND AGENCIES DEVELOPING LOW-LEVEL COUNTING TECHNIQUES

AUSTRALIA
- Australian Atomic Energy Commission, Sutherland, Sydney
- Australian National University, Canberra

AUSTRIA
- International Atomic Energy Agency, Vienna
- Atominstitute de Östereichischen Universitäten, Wien
- United Research Inst. Arsenal, Vienna
- Austrian Environment Protection Agency,
- Department of Radiation Protection, Vienna

BELGIUM
- Central Bureau for Nuclear Measures, Geel
- State University of Gent, Gent
- Belgian Nuclear Centre, Mol

BULGARIA
- Radiochemical Laboratory, Faculty of Chemistry, University of Sofia, Sofia
- Institute of Nuclear Research and Nuclear Energy, Bulgarian Academy of Sciences, Sofia

CANADA
- Radiation Protection Laboratory, Ontario Ministry of Labour. Rexdale, Ontario
- Département de Chimie, Université Laval, Cité Universitaire, Québec
- National Water Research Institute, Environment Canada, Burlington
- Lepton Laboratory, Dept. of Physics, University of Guelph, Guelph, Ontario
- Isotrace Laboratory, Dept. of Physics, University of Toronto, Toronto, Ontario

CROATIA
- Institute Rudjer Boskovic, Zagreb
- University of Osijek, Faculty of Education, Osijek

CZECHOSLOVAKIA
- Comenius University, Department of Nuclear Physics Bratislava
- Research Institute of Nuclear Power Stations, Jaslovske Bohunice
- Institute of Hygiene and Epidemiology, Prague
- Institute of Radioecology and Nuclear Techniques, Kosice

DENMARK
- Riso National Laboratory, Roskilde

FINLAND
- Walac Oy, Turku
- University of Helsinki, Department of Physics, Helsinki

FRANCE
- Laboratoire René Bernas, Centre de Spectrométrie Nucléaire et de Spectrométrie de Masse, Orsay
- Centre d'Etudes Nucléaires de Saclay, Gif-sur-Yvette
- CNRS-CEA Centre de Faibles Radioactivités, Gif-sur-Yvette

GEORGIA
- Tbilisi State University, Dept. of Nuclear Physics, Tbilisi

GERMANY
- Zentralinstitute für Kernforschung, Rossendorf
- Academy of Mining, Department of Physics, Freiburg
- Max-Planck-Institut fur Kernphysik, Heidelberg
- Heidelberg Universität, Institu t für Umweltforschung, Heidelberg
- Institut für Strahlenshutz, Neuherberg
- Fakultat für Physik, München Technische Universität, Garching

GRECE
- Nuclear Research Center "Democritos", Athens

HUNGARY
- Central Institute for Physics, Budapest
- Institute of Nuclear Research, Debrecen
- University of Debrecen, Institute of Experimental Physics, Debrecen
- Institute of Isotopes, Budapest
- National Office of Measures, Budapest

INDIA
- Tata Institute of Fundamental Research, Bombay
- Bhabha Atomic Research Centre, Bombay
- Physical Research Laboratory, Ahmedabad

ICELAND
- Reykyavik University, Institute of Physics, Reykyavik

ITALY
- Milano University, Department of Physics, Milano
- University of Roma, Institute of Physics, Roma

JAPAN	- Institute of Nuclear Study, Tokyo University, Tokyo - Japan Atomic Energy Research Institute, Ibaraki-ken - Low-Level Radioactivity Laboratory, Kanazawa University, Wake, Tatsunokuchi
MONACO	- International Laboratory of Marine Radioactivity, Monaco
NETHERLAND	- University of Groningen, Physics Laboratory, Groningen
NEW ZEALAND	- Institute of Nuclear Sciences, Lower Hutn
NORWAY	- Norwegian Institute of Technology, Radiological Dating Laboratory, Trondheim
POLAND	- Laboratory for Radiological Protection, Warszawa - Atomic Energy Institute, Swierk-Otwock - Silesian Technical University, Gliwice - Institute of Physics and Nuclear Techniques, Crakow
ROMANIA	- Institute of Atomic Physics, Bucharest
RUSSIA	- Institute for Nuclear Research, Moscow - V.I.Vernadsky Institute of Geochemistry, Moscow - A.F.Joffe Physical-Technology Institute, St. Petersburg - Joint Institute for Nuclear Research, Flerov Laboratory of Nuclear Reactions, Dubna
SLOVENIA	- Josef Stefan Institute, Ljubljana
SPAIN	- Seville University, Faculty of Physics, Seville
SWEDEN	- University College of Sundvall, Department of Physics, Sundvall - National Defence Research Institute, Stockholm - University of Uppsala, Institute of Physics, Uppsala
SWITZERLAND	- University of Bern, Institute of Physics, Bern - Institut für Mittelenergie Physik, ETH-Honggerberg, Zürich
UK	- National Radiological Protection Laboratory Board, Chilton, Didcot - Scottish Universities Research and Reactor Centre, Glasgow - Atomic Energy Research Establishment, Harwell - National Physical Laboratory, Teddington Middx
UKRAINE	- Institute of Nuclear Studies, Kiev
USA	- University of Miami, Rosential School of Marine and Atmospheric Science, Miami, Florida - Naval Research Laboratory, Washington, D.C. - Oak Ridge National Laboratory, Oak Ridge, Tennessee - National Institute of Standards and Technology, Washington, D.C. - University of Rochester, Nuclear Structure Research Laboratory, Rochester, N.Y. - Environmental Measures Laboratory, US Department of Energy, New York, N.Y. - Radiological and Environmental Sciences Laboratory, Idaho Falls, Idaho - Pacific Northwest Laboratory, Richland, Washington - Argonne National Laboratory, Physics Division, Argonne, Illinois
YUGOSLAVIA	- Institute of Nuclear Sciences, Belgrade

7. REFERENCES

1. H. Oeschger and M.Wahlen, in: Ann. Rev. Nucl. Sci. 25, 423 (1975).
2. Proc. Internat. Symp. Low Level Counting Spectrometry, West Berlin, 1981. IAEA, Vienna (1981).
3. J.M.R.Hutchison et al., Nucl. Instr. Meth. 112, 30 (1973).
4. 1st Internat. Conf. Low Level Measurements of Actinides and Long Lived Radionuclides in Biological and Environment.Samples, Lund, 1986. J. Radioanal. Nucl. Chem. Articles 115, Nos.1,2.(1987).
5. 5th Symp. Environment. Radiochem. Analysis, Harwell,1986. Sci.Total Environm. 69 (1988).
6. Proc. 1st Internat. Conf. Low Level Counting, High Tatras, 1975. P.Povinec and S.Usacev Eds. SNP, Bratislava (1977).
7. Proc. 2nd Internat. Conf. Low Level Counting, High Tatras, 1980. P.Povinec Ed. Vols. 1,2, Veda, Bratislava (1982).
8. Proc. 3rd Internat. Conf. Low Level Counting; short contributions. Bratislava, 1985. P.Povinec Ed. Veda, Bratislava (1987).
9. Proc. 3rd Internat. Conf. Low Level Counting, Bratislava, 1985; plenary lectures. Nucl. Instr. Meth. Phys. Res. B17, Nos.5,6, pp. 377-570 (1986).
10. F. Schonhofer and E. Henrich, J. Radioanal. Nucl. Chem. Articles 115, 317 (1987).
11. G. Hut, Nucl. Instr. Meth. Phys. Res. B17, 475 (1986).
12. A.E. Litherland, Nucl. Instr. Meth. Phys. Res. B5, 10 (1984).
13. W. Kutchera, Nucl. Instr. Meth. Phys. Res. B17, 377 (1986).
14. J.P.F. Sellschop, Nucl. Instr. Meth. Phys. Res. B29, 439 (1989)..
15. J.V. Melikov, Experimental Methods in Nuclear Physics (in Russian), Izd. MGU, Moscow (1973).
16. P. Povinec et al., Applied Nuclear Physics (in Slovak), Comenius University Bratislava (1985).
17. N.A. Vartanov and P.S. Samojlov, Applied Scintillation Gamma-Spectrometry (in Russian). Atomizdat, Moscow (1975).
18. V. Randa et al., Non-Destructive Neutron Activation Analysis III. Nucl. Inform. Centre, Prague (1979).
19. P. Povinec et al., Int. J. Appl. Rad. Isotopes 32, 720 (1981).
20. J.C. Roy et al., J. Radioanal. Nucl. Chem. Articles 130, 221 (1989).
21. J.H. Reeves and R.J.Arthur, J. Radioanal. Nucl. Chem. Articles 124, 435 (1988).
22. R.L. Brodzinski et al., J. Radioanal. Nucl. Chem. Articles 124, 513 (1988); Nucl. Instr. Meth. Phys. Res. A239, 207 (1985).
23. M. Wojcik, Nucl. Instr. Meth. 189, 645 (1981).
24. H.L. Malm et al., Nucl. Instr. Meth. Phys. Res. 223, 420 (1984).
25. S. Unterricker et al., Isotopenpraxis 25, 247 (1989).
26. O.P. Sobornov, Atomnaya energiya 50, 43 (1981).
27. J. Stanicek et al., in Ref. 8, p. 131.
28. M. Chudy et al., in Ref. 7, Vol.1, p.255.
29. G. Heuser, Nucl. Instr. Meth. Phys. Res. B17, 411 (1986).
30. H.H. Loosli et al., Nucl. Instr. Meth. Phys. Res. B17, 402 (1986).
31. W. Helbig and S. Niese, Nucl. Instr. Meth. Phys. Res. B18, 431 (1986);J.Radioanal. Nucl. Chem. Articles 100, 155 (1986).
32. D. Heberd et al., Nucl. Instr. Meth. Phys. Res. B17, 427 (1986).
33. Y.G. Zdesenko et al., in Ref.8, p. 15.
34. A.A. Pomansky, Nucl. Instr. Meth. Phys. Res. B17, 406 (1986).
35. A. Allesandrello et al., Nucl.Instr.Meth.Phys.Res. B17, 411 (1986).
36. Y. Termonia and J. Deltour, J. Phys. D7, 2157 (1974).
37. D.E.Watt, D.Ramsden, High Sensitivity Counting Techniques, Pergamon Press, Oxford (1964).
38. I. Bucina and I. Malatova, in Ref. 8, p.49.
39. L.A. Currie, Anal. Chem. 40, 586 (1968).
40. B. Altschuler and B. Pasternack, Health Phys. 9, 293 (1963).
41. D.F. Covell, Anal. Chem. 31, 1785 (1959).
42. J.A. Cooper, Nucl. Instr. Meth. 82, 273 (1970); 94, 289 (1971).
43. R.W.Fink, NBS spec. publ. 604 , 5 (1981).
44. C.M.Lederer et al., Table of Isotopes. Wiley, New York (1978).

45. R.G. Helmer, Int. J. Appl. Radiat. Isotopes 34, 1105 (1983).
46. K. Debertin and U. Schotzig, Nucl. Instr. Meth. 158, 471 (1979).
47. D.D. Hoppes et al., NBS spec. publ. 626, 85 (1982).
48. Y. Takeda et al., Nucl. Instr. Meth. 136, 369 (1976).
49. F. Hajnal. K. Klusek, Nucl. Instr. Meth. 122, 659 (1974).
50. S. Gmuca and I. Ribanski, Nucl. Instr. Meth. 202, 435 (1982).
51. R.S. Seymour et al., J. Radioanal. Nucl. Chem. Articles 123, 529 (1988).
52. H. Baba et al., Nucl. Instr. Meth. A309, 236 (1991).
53. O. Slavik, in Ref. 8, p.173.
54. N.H. Cutshall, I.L. Larsen and C.R. Olsen, Nucl. Instrum. Meth. 206, 309 (1983).
55. S.R. Joshi, Appl. Rad. Isot. 40, 691 (1989).
56. S.R. Joshi, J. Radioanal. Nucl. Chem. Articles 116, 169 (1987).
57. K. Debertin and J. Ren, Nucl. Instr. Meth. Phys. Res. A278, 541 (1989).
58. L. Zikovsky, J. Radioanal. Nucl. Chem. Articles 132, 153 (1989).
59. H.A. Helms, Semiconductor Radiation Detectors, PGT Europa GmbH; prospect.
60. J.A.Cooper and R.W. Perkins, Nucl. Instr. Meth. 99, 125 (1972).
61. H.A. Das, J. Radioanal. Nucl. Chem. Articles 115, 159 (1987); ibidem 114, 207 (1987).49.
62. P.J.Nolan et al., Nucl. Instr. Meth. A236, 95 (1985).
63. G. Beseova et al., in Ref.7, Vol.2, 9.125.
64. G. Heuser et al., in Ref.7, Vol.1, p.127.
65. P. Povinec, Isotopenpraxis 18, 423 (1982).
66. K. Nogami et al., Nucl. Instr. Meth, 150, 195 (1978).
67. J. Szarka, K. Janko, in Ref. 8, p.169.
68. P. Rizzacassa, Nucl. Instr. Meth. Phys. Res. B17, 519 (1986).
69. A. Rytz, Atomic Nucl. Data Tables 47, 205 (1991).
70. J.C. Post, Actinide Reviews 1, 55 (1967).
71. L.C. Northcliffe and R.F.Schilling, Nucl. Data Tables A7, 233 (1970)
72. F. Hubert et al., Ann. Phys. Suppl. 5, 1 (1980).
73. D. Srdoc, in Ref.7, Vol.1, p.305.
74. C.W. Sill and D.G. Olsen, Anal. Chem. 42, 1596 (1970).
75. S. Saro, in Ref. 7, Vol.1, p.231.
76. F. Schonhofer et al., J. Radioanal. Nucl. Chem. 115, 125 (1987).
77. A.P. Fews and D.L. Henshow, Nucl. Instr. Meth. 197, 517 (1982).
78. A.N. Kuznetsov et al., Pribory Teknika Exper. 36 (1987).
79. T. Hashimoto and Y. Sakai, J. Radioanal. Nucl. Chem. Articles 138, 195 (1990).
80. M.I. Yakunin, in Applied Nuclear Spectroscopy, Vol. 5, p. 117 (in Russian). Atomizdat, Moscow (1975).
81. M.I. Ivanov et al., JINR Commun. 13-82-860, Dubna (1982).
82. S.A.Ch. Hogberg et al., Nucl. Instr. Meth. 113, 573 (1973).
83. V.M. Gorbachev et al., Basic Characteristics of Isotopes of Heavy Elements (in Russian), Atomizdat, Moscow (1975).
84. N.Holden and D.C. Hoffman, Report BNL 46463, Brookhaven (1991).
85. V.E. Viola et al., Phys. Rev. C31, 1550 (1985).
86. J.M. Alexander and M.T. Gazdik, Phys. Rev. 120, 874 (1960).
87. G.N. Flerov and G.M. Ter-Akopian, Pure Appl. Chem. 53, 909 (1981).
88. G.N. Flerov et al., JINR Rep. D6-4554, Dubna (1969); Yadernaya Fizika 20, 472 (1974).
89. E.A. Sokol et al., Nucl. Instr. Meth. A245, 481 (1986).
90. E. Cheifetz et al., Phys. Rev. C6, 1348 (1972).
91. G.M. Ter-Akopian et al., Nucl. Instr. Meth. 190, 119 (1981).
92. R.L. Macklin et al., Nucl. Instr. Meth. 102, 181 (1972).
93. J.C. Barton et al., J. Phys. G: Nucl. Part. Phys. 17, 1885 (1991).
94. K. Behringer et al., Phys. Rev. C9, 48 (1974).
95. R.L. Fleischer et al., Nuclear. Tracks in Solids. UC Press, Berkeley (1975).
96. Yu.P. Gangrsky et al. Detection and Spectrometry of Fission Fragments (in Russian). Energoizdat, Moscow (1981).
97. C. Arpesella, Nucl. Instr. Meth. Phys. Res. A277, 1 (1989).